Supplemental material to this article can be found at:
http://jpet.aspetjournals.org/content/suppl/2022/02/02/jpet.121.001000.DC1

1521-0103/381/1/54–66$35.00
THE JOURNAL OF PHARMACOLOGY AND EXPERIMENTAL THERAPEUTICS
Copyright © 2022 by The American Society for Pharmacology and Experimental Therapeutics
dx.doi.org/10.1124/jpet.121.001000
J Pharmacol Exp Ther 381:54–66, April 2022

The Journal of PHARMACOLOGY And Experimental Therapeutics

Opportunities for Precision Treatment of *GRIN2A* and *GRIN2B* Gain-of-Function Variants in Triheteromeric N-Methyl-D-Aspartate Receptors

Wei Han[1], Hongjie Yuan, James P. Allen, Sukhan Kim, Gil H. Shaulsky, Riley E. Perszyk, Stephen F. Traynelis, and Scott J. Myers

Department of Pharmacology and Chemical Biology (W.H., H.Y., J.P.A., S.K., G.H.S., R.E.P., S.F.T., S.J.M.) and Center for Functional Evaluation of Rare Variants (CFERV), Emory University School of Medicine, Emory University, Atlanta, Georgia (W.H., H.Y., J.P.A., S.K., G.H.S., S.F.T., S.J.M.)

Received October 29, 2021; accepted January 7, 2022

ABSTRACT

N-methyl-D-aspartate receptors (NMDARs) are tetrameric assemblies of two glutamate N-methyl-D-aspartate receptor subunits, GluN1 and two GluN2, that mediate excitatory synaptic transmission in the central nervous system. Four genes (*GRIN2A-D*) encode four distinct GluN2 subunits (GluN2A-D). Thus, NMDARs can be diheteromeric assemblies of two GluN1 plus two identical GluN2 subunits, or triheteromeric assemblies of two GluN1 subunits plus two different GluN2 subunits. An increasing number of *de novo GRIN* variants have been identified in patients with neurologic conditions and with *GRIN2A* and *GRIN2B* harboring the vast majority (> 80%) of variants in these cases. These variants produce a wide range of effects on NMDAR function depending upon its subunit subdomain location and additionally on the subunit composition of diheteromeric versus triheteromeric NMDARs. Increasing evidence implicates triheteromeric GluN1/GluN2A/GluN2B receptors as a major component of the NMDAR pool in the adult cortex and hippocampus. Here, we explore the ability of GluN2A- and GluN2B-selective inhibitors to reduce excess current flow through triheteromeric GluN1/GluN2A/GluN2B receptors that contain one copy of *GRIN2A* or *GRIN2B* gain-of-function variants. Our data reveal a broad range of sensitivities for variant-containing triheteromeric receptors to subunit-selective inhibitors, with some variants still showing strong sensitivity to inhibitors, whereas others are relatively insensitive. Most variants, however, retain sensitivity to non-selective channel blockers and the competitive antagonist D-(-)-2-amino-5-phosphonopentanoic acid. These results suggest that with comprehensive analysis, certain disease-related *GRIN2A* and *GRIN2B* variants can be identified as potential targets for subunit-selective modulation and potential therapeutic gain.

SIGNIFICANCE STATEMENT

Triheteromeric NMDA receptors that contain one copy each of the GluN2A and GluN2B subunits show intermediate sensitivity to GluN2A- and GluN2B-selective inhibitors, making these compounds candidates for attenuating overactive, *GRIN* variant-containing NMDA receptors associated with neurological conditions. We show that functional evaluation of variant properties with inhibitor pharmacology can support selection of a subset of variants for which GluN2 subunit-selective agents remain effective inhibitors of variant-containing triheteromeric NMDA receptors.

Introduction

N-methyl-D-aspartate receptors (NMDAR) are ligand-gated ion channels that mediate a slow, Ca^{2+}-permeable component of excitatory synaptic transmission (MacDermott et al., 1986; Hansen et al., 2021). NMDARs can be blocked by extracellular Mg^{2+} in a voltage-dependent manner (Mayer et al., 1984; Nowak et al., 1984) and play a key role in many processes in the central nervous system, including learning, memory, and neuronal development (Hansen et al., 2021). NMDAR dysfunction has been suggested to be involved in various neurologic and neuropsychiatric disorders such as epilepsy, intellectual disability, autism spectrum disorder, neuropathic pain, depression, Parkinson's disease, and schizophrenia (Lau and Zukin,

[1]Current affiliation: Department of Neurology, Children's Hospital of Chongqing Medical University, Chongqing, China.

This work was supported by the National Institutes of Health National Institute of Neurologic Disorders and Stroke [Grant NS111619] (S.F.T.), the National Institute of Mental Health [Grant MH127404] (H.Y.), the Eunice Kennedy Shriver National Institute of Child Health and Human Development [Grant HD082373] (H.Y.), and the National Institute on Aging [Grant AG072142] S.J.M.

H.Y., S.J.M., and S.F.T. are co-inventors of Emory-owned intellectual property. S.F.T. is a PI on research grants from Biogen and Janssen to Emory, is a member of the SAB for Sage Therapeutics, Eumentis Therapeutics, the GRIN2B Foundation, and the CureGRIN Foundation. H.Y. is the PI on a research grant from Sage Therapeutics to Emory. S.F.T. and S.J.M. own stock in a company (NeurOp, Inc.) that is developing a GluN2B antagonist.

dx.doi.org/10.1124/jpet.121.001000.

ABBREVIATIONS: CI, confidence interval; cRNA, ribonucleic acid made from cDNA; D-APV, D-(-)-2-amino-5-phosphonopentanoic acid; GoF, gain of function; GluN1, the 1 subunit of the glutamate N-methyl-D-aspartate receptor; GluN, the subunit of the glutamate N-methyl-D-aspartate receptor; NAM, negative allosteric modulator; NMDA, N-methyl-D-aspartate; NMDAR, N-methyl-D-aspartate receptor; NTD, amino terminal domain; WT, wild-type.

Downloaded from jpet.aspetjournals.org at ASPET Journals on April 19, 2024

2007; Mony et al., 2009; Traynelis et al., 2010; Hansen et al., 2021).

The NMDAR receptors are encoded by the *GRIN* gene family, which includes *GRIN1*, *GRIN2A-D*, and *GRIN3A-B* genes. Whereas in vitro studies on recombinant receptors have largely been conducted with diheteromeric NMDARs that contain two copies of the same subunit of the glutamate N-methyl-D-aspartate receptor (GluN2) subunit co-assembled with two copies of GluN1 expressed in either *Xenopus* oocytes or transfected mammalian cell lines (Traynelis et al., 2010; Paoletti et al., 2013), a large fraction of NMDARs expressed in vivo are triheteromeric assemblies of two GluN1 subunits and two different GluN2 subunits in the tetrameric complex. For example, GluN1/GluN2A/GluN2B comprise over half of the NMDARs in the adult cortex and hippocampus (Sheng et al., 1994; Luo et al., 1997; Al-Hallaq et al., 2007; Rauner and Kohr, 2011; Tovar et al., 2013). Moreover, different combinations of GluN2 subunits assemble into the receptor complex in distinct brain regions (Rauner and Köhr, 2011; Tovar et al., 2013; Hansen et al., 2014; Hansen et al., 2021). Recent evidence has shown that the kinetic and pharmacological properties of GluN1/GluN2A/GluN2B triheteromeric receptors are distinct from the GluN1/GluN2A or GluN1/GluN2B diheteromeric receptors (Hansen et al., 2014; Stroebel et al., 2014; Bhattacharya et al., 2018; Yi et al., 2019). However, the biophysical and pharmacological properties of triheteromeric GluN2A- and GluN2B-containing NMDARs are strongly influenced by GluN2A (Hansen et al., 2014), whereas neither GluN2B nor GluN2D dominate the properties of GluN1/GluN2B/GluN2D triheteromeric NMDA receptors (Yi et al., 2019).

Whole exome sequencing has identified a large number of rare *do novo GRIN* variants associated with neurologic disorders (Burnashev and Szepetowski, 2015; Yuan et al., 2015; Hu et al., 2016; Li et al., 2016; Swanger et al., 2016; XiangWei et al., 2018, 2019; Myers et al., 2019; Strehlow et al., 2019; Benke et al., 2021), with *GRIN1*, *GRIN2A*, *GRIN2B*, and *GRIN2D* genes being highly intolerant to genetic variation. As a result, a large number of missense *GRIN2A* and *GRIN2B* variants have been identified in patients with various neurologic conditions. These variants cluster in select regions of the subunit, such as the amino terminal domain (NTD), the agonist binding domain (ABD), the transmembrane domains (TMD), and the linker regions connecting these subdomains (Yuan et al., 2014; Chen et al., 2017; Ogden et al., 2017; Perszyk et al., 2020, 2021; Hansen et al., 2021). Variants localized in these subdomains can drive unique electrophysiological effects and thus distinct neurologic phenotypes in patients (XiangWei et al., 2018; Strehlow et al., 2019). Here, we investigate the utility of potential therapeutic agents for treatment of rare *GRIN* variants. We focused on gain-of-function (GoF) variants that increase current flow in *GRIN2A* and *GRIN2B* in the context of triheteromeric NMDAR complexes that include a single subunit that harbors the damaging rare variant, since this more likely reflects the NMDAR context in vivo. Prior studies showed that the GluN2B allosteric inhibitor radiprodil, which can reduce seizure burden in patients with infantile spasms (Auvin et al., 2020), inhibits diheteromeric GluN2B receptors harboring two copies of rare GluN2B de novo GoF variants (Mullier et al., 2017). Other GluN2B inhibitors that occupy the same binding site as radiprodil inhibit triheteromeric GluN1/GluN2A/GluN2B receptors with lower potency and diminished maximal inhibition at saturating inhibitor concentrations (Hansen et al., 2014; Yi et al., 2019). This raises the question of how sensitive triheteromeric GluN1/GluN2A/GluN2B receptors harboring GoF variants are to GluN2B-selective inhibitors. A similar question arises concerning the sensitivity of variant-containing triheteromeric receptors to the GluN2A-selective inhibitor, TCN-201 (Bettini et al., 2010).

Here, we evaluated the actions of three classes of NMDAR inhibitors on triheteromeric GluN1/GluN2A/GluN2B receptors that contain a single damaging variant: subunit-selective negative allosteric modulators (NAMs), channel blockers, and the competitive antagonist, D-(-)-2-amino-5-phosphonopentanoic acid (D-APV). Because most GoF variants are localized in the linker and TMDs of GluN2A and GluN2B NMDAR subunits, we selected a representative set of variants from these regions for study. Our results show that distinct subdomain variants have divergent responses to NMDAR inhibitors. Among these drug classes, channel blockers and D-APV were capable of attenuating the subset of variants we studied in triheteromeric receptors that contain one copy of the mutant allele, whereas the subunit selective NAMs showed variable effects that were dependent on the specific genetic variant.

Materials and Methods

Drugs and Reagents. Radiprodil, ifenprodil, CP-101,606, Ro 25-6981, and TCN-201 were purchased from Axon MedChem (Reston, VA USA), memantine and dextromethorphan from Sigma Aldrich (USA), and ketamine from Hospira, Inc. (Lake Forest, IL). Stock concentrations of each compound were prepared in deionized water (memantine and ketamine), DMSO (dextromethorphan, radiprodil, ifenprodil, CP-101,606, Ro 25-6981, and TCN-201); the 100 mg/ml ketamine stock solution contained 0.1 mg/ml of benzethonium chloride. After dilution into oocyte perfusion media, the final DMSO concentration was 0.1% (v/v).

cDNAs and Molecular Biology. Wild-type (WT) rat cDNAs for GluN1-1a (GenBank accession numbers U08261 for GluN1 lacking exon5 but containing exons 21 and 22), GluN2A (GenBank accession number D13211), and GluN2B (GenBank accession number U11419) were subcloned into the pCI-neo mammalian expression vector. The constructs of triheteromeric receptors were generated using rat GluN1 and GluN2A with modified C-terminal peptide tags as previously described (Hansen et al., 2014). Briefly, C-terminal peptide tags were generated from the leucine zipper motifs found in $GABA_{B1}$ (referred to as C1) and $GABA_{B2}$ (referred to as C2). These tags were placed downstream of a synthetic helical linker and upstream of a KKTN endoplasmic reticulum retention signal (Jackson et al., 1990, 1993; Zerangue et al., 2001). The C1 and C2 leucine zipper motifs can enter into a coiled-coil interaction that will mask the KKTN retention motif and allow expression of mature receptors on the cell surface. The tag was introduced in frame and in place of the stop codon at the GluN2A C-terminal tail (to make $2A_{C1}$ and $2A_{C2}$). A chimeric GluN2B subunit was constructed in which the 2B carboxyl tail after residue 838 was replaced by the GluN2A carboxyl tail and C-terminal-linker-C1 or -C2-ER retention motifs (to make $2B_{AC1}$ and $2B_{AC2}$, hereafter called $2B_{C1}$ and $2B_{C2}$, respectively), as described by Hansen et al. (2014). The efficiency of the peptide tags for controlling surface expression could be assessed through the measurement of the "escape" currents estimated using a pair of mutations that rendered the agonist binding domain incapable of binding glutamate and thus unable to pass current. These mutations were GluN2A-R518K,T690I and GluN2B-R519K,T691I.

Rare human *GRIN2A* (E551K, P552R, S644G, L649V, L812M, M817V) or *GRIN2B* (G543R, A639V, M818T, A819T) NMDAR variants were introduced into their respective rat cDNAs using a QuikChange

Downloaded from jpet.aspetjournals.org at ASPET Journals on April 19, 2024

mutagenesis protocol (Agilent, USA) according to the manufacturer's instructions. After introduction of the genetic variant into the cDNA, the full open reading frame was sequence-verified (Sanger method, Eurofins, KY USA) to ensure only the intended genetic variant was introduced into the cDNA. The cDNA was then linearized with the Not I restriction enzyme and ribonucleic acid made from cDNA (cRNA) synthesized according to the manufacturer's instructions using T7 RNA polymerase with mMessage mMachine (Invitrogen, USA).

Triheteromeric Three-Dimensional Missense Tolerance Determination. To determine three-dimensional missense tolerance (3DMTR, Perszyk et al., 2021) of the GluN1/GluN2A/GluN2B, we used the recently published cryo-EM structure of the triheteromeric NMDAR (PDB: 5UOW, Lü et al., 2017). This cryo-EM structure was determined using the *Xenopus laevis* analog subunits, so, in using the 3DMTR application (https://github.com/riley-perszyk/3DMTR), the *Xenopus laevis* grin1.L, grin2a.L, and grin2b gene sequences were used with the human *GRIN1*, *GRIN2A*, and *GRIN2B* sequences (NM_001185090.2_, NM_000833.5, and NM_000834.5, respectively) to align the gnomAD (version 2.1.1) missense and samesense variant entries for each gene.

Oocyte Preparation and Injections. Stage V-VI *Xenopus laevis* oocytes were prepared from commercially available ovaries (Xenopus 1 Inc., Dexter MI, USA). Briefly, the ovary was digested with Collagenase Type 4 (Worthington-Biochem) solution in Ca^{2+}-free modified Barth's solution, which contained (in mM) 88 NaCl, 2.4 $NaHCO_3$, 1 KCl, 0.82 $MgSO_4$, and 10 (4-(2-hydroxyethyl)-1-piperazineethanesulfonic acid) (pH 7.4 with NaOH) and was supplemented with 1 U/ml of penicillin-streptomycin (Gibco #15140122). The ovary was incubated with gentle shaking at room temperature (23°C) for 2 hours, rinsed ten times (10 minutes each) with fresh Ca^{2+}-free Barth's solution, and then rinsed four times (5 minutes each) with normal Barth's solution that contained (in mM) 88 NaCl, 2.4 $NaHCO_3$, 1 KCl, 0.33 $Ca(NO_3)_2$, 0.41 $CaCl_2$, 0.82 $MgSO_4$, and 10 (4-(2-hydroxyethyl)-1-piperazineethanesulfonic acid), adjusted to pH 7.4 with NaOH and supplemented with 100 μg/ml of gentamycin and 1 U/ml of penicillin-streptomycin. The prepared and sorted oocytes were then incubated in normal Barth's solution prior to, and after, injections. cRNAs encoding GluN1, as well as C1- and C2-tagged GluN2A or GluN2B were expressed as previously described (Strong et al., 2021). Briefly, GluN1:$GluN2_{C1}$:$GluN2_{C2}$ cRNAs were injected at a 1:2:2 ratio with ~10 ng of total cRNA in a total volume of 50 nl to achieve the following combinations of subunit RNA: GluN1:$GluN2A_{C1}$:$GluN2A_{C2}$ or GluN1:$GluN2B_{C1}$:$GluN2B_{C2}$ to generate diheteromeric receptors, or GluN1:$GluN2A_{C1}$:$GluN2B_{C2}$, GluN1:$GluN2A_{C1}$-(variant):$GluN2B_{C2}$, or GluN1:$GluN2A_{C1}$:$GluN2B_{C2}$-(variant) to make WT or variant-containing triheteromeric NMDARs. Injected oocytes were incubated at 15–19°C in Barth's solution for 1 to 3 days before recording.

Two-Electrode Voltage Clamp Recordings. Two-electrode voltage clamp recordings were made at 22–23°C 1—3 days after injection using OC725C amplifiers (Warner Instruments, Hamden, CT) similarly to that previously described (Strong et al., 2021). The recording solution contained (in mM) 90 NaCl, 1 KCl, 10 (4-(2-hydroxyethyl)-1-piperazineethanesulfonic acid), 0.5 $BaCl_2$, and 0.01 EDTA and was adjusted to pH 7.4 with NaOH. Recording electrodes were filled with 0.3 – 3.0 M of KCl. Oocytes were perfused in recording solution supplemented with agonists or drugs as indicated, and the membrane was clamped at -40 mV. For single concentration drug inhibition experiments, test currents were recorded in response to maximal glutamate and glycine (100 μM each) and then also with the inhibitor at 3 μM (ifenprodil, radiprodil, Ro 25-6981, CP-101,606, TCN-201) for 3—6 minutes. Concentration-response curves were determined similarly but with increasing concentrations of the GluN2B negative allosteric modulators; TCN-201 was co-applied with 100 μM glutamate and 3 μM glycine. Drug concentration-response curves were obtained until steady state inhibition was obtained at each concentration, typically 3–6 minutes. Drug concentration-response curves with the uncompetitive channel blockers memantine, ketamine, and dextromethorphan were conducted similarly, except each drug concentration was applied for 1 minute to reach steady-state.

For drug inhibition studies, oocyte recordings were made from 2 or more independent experiments (i.e., oocyte injection cycles) when testing inhibitors against variant-containing triheteromeric NMDARs and WT controls. Drug potency was quantified as the concentration that inhibits 50% of the current for each oocyte by fitting Eq. (1) to the concentration-response data:

$$\%\text{Response} = (100 - \text{minimum})/\left(1 + \left([\text{concentration}]/\text{IC}_{50}\right)^{\text{nH}}\right) + \text{minimum} \quad (1)$$

where *minimum* is the residual response in saturating concentration of the inhibitor (constrained to be >0), IC_{50} is the concentration of inhibitor that causes half-maximal inhibition, and *nH* is the Hill slope. For channel blockers, minimum was constrained to be equal to or greater than 0.

In experiments testing the effects of the competitive antagonist D-APV, the glutamate concentrations were adjusted to the EC_{50} values as determined for the variant triheteromeric receptors as shown in Supplemental Table S2. Here, glutamate agonist potency was quantified as the concentration that elicited half-maximal activation of the current response for each oocyte by fitting Eq. (2) to the concentration-response data:

$$\%\text{Response} = \left([\text{concentration}]^{\text{nH}}\right)/\left([\text{concentration}]^{\text{nH}} + \text{EC}_{50}{}^{\text{nH}}\right) \quad (2)$$

where *concentration* is the concentration of the agonist, EC_{50} is the concentration of agonist that causes half-maximal activation, and *nH* is the Hill slope.

The uncompetitive channel blockers memantine (100 μM), ketamine (100 μM), and dextromethorphan (300 μM), and the NTD-site negative allosteric modulator radiprodil (3 μM) were also tested for inhibition at different membrane potentials by stepping the oocyte membrane potential in 10 mV increments from -90 mV to +30 mV in the absence

TABLE 1
Summary of *GRIN* variants and phenotype information

#	Gene	Mutation	Genotype	Location	Origin	Phenotype	Source or Reference
1	*GRIN2A*	p.E551K	c.1651G>A	Pre-M1	de novo	Epi/DD	Clinvar VCV000520918.2
2	*GRIN2A*	p.P552R	c.1655C>G	Pre-M1	de novo	Epi/DD	Ogden et al., 2017
3	*GRIN2A*	p.S644G	c.1930A>G	M3	de novo	Epi/DD	Amador et al., 2020
4	*GRIN2A*	p.L649V	c.1945C>G	M3	de novo	Epi/ID	De Ligt et al., 2012
5	*GRIN2A*	p.L812M	c.2434C>A	Pre-M4	de novo	EE	Yuan et al., 2014
6	*GRIN2A*	p.M817V	c.2449A>G	M4	de novo	Epi/DD	Chen et al., 2017
7	*GRIN2B*	p.G543R	c.1627G>A	Pre-M1	de novo	CND	ClinVar VCV000984886
8	*GRIN2B*	p.A639V	c.1916C>T	M3	de novo	DD/MCD	Helbig et al., 2016
9	*GRIN2B*	p.M818T	c.2453T>C	M4	de novo	Epi/DD	Platzer et al., 2017
10	*GRIN2B*	p.A819T	c.2455G>A	M4	de novo	Epi/DD	Platzer et al., 2017

DD, developmental delay; Epi, epilepsy; EE, epileptic encephalopathy; ID, intellectual disability; MCD, malformation of cortical development; CND, complex neurodevelopmental disorder.

Downloaded from jpet.aspetjournals.org at ASPET Journals on April 19, 2024

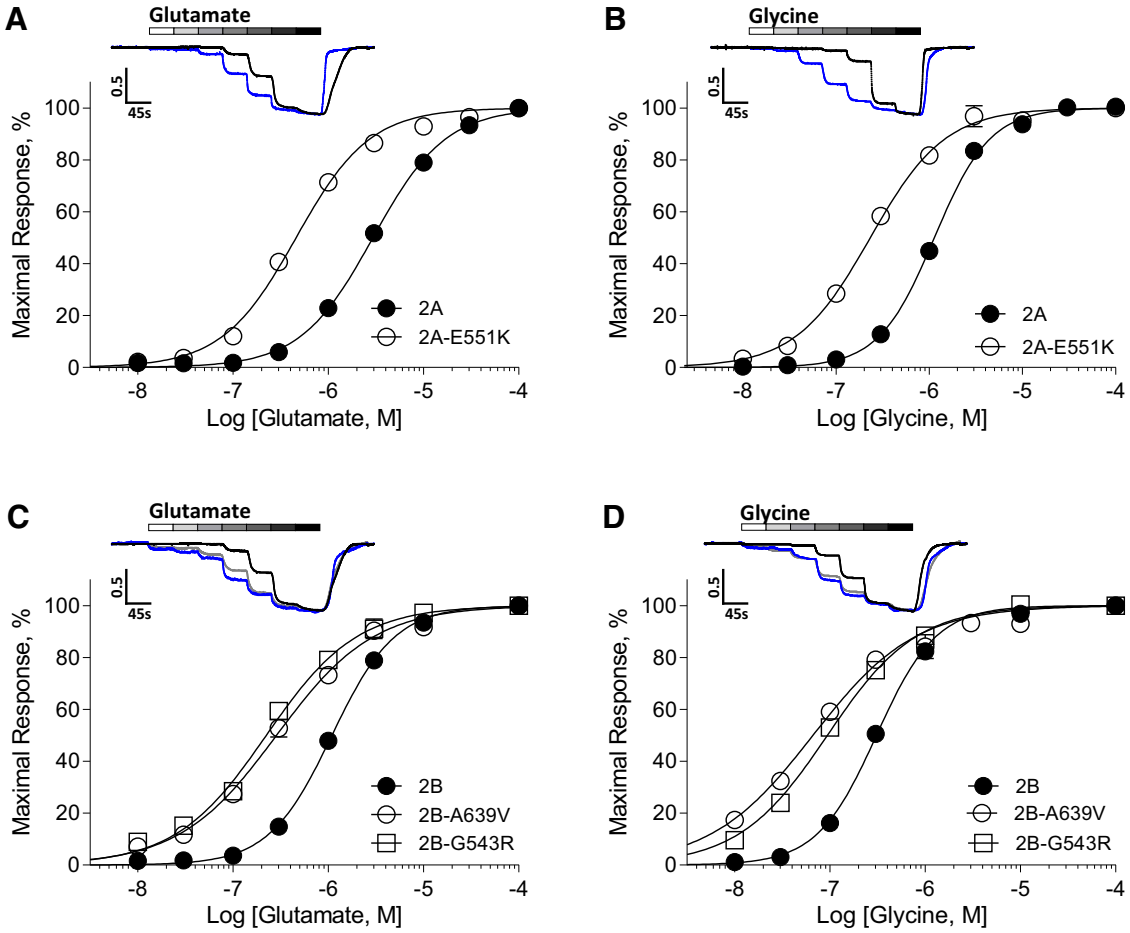

Fig. 1. Agonist potency for *GRIN2A*-E551K, *GRIN2B*-A639V, and *GRIN2B*-G543R variants expressed as diheteromeric N-methyl-D-aspartate receptors. (A–B) Concentration-response curves for glutamate (panel A) and glycine (panel B) activation of GluN1/GluN2A-E551K (open circles) and wild-type (WT) GluN1/GluN2A (black circles) receptors. Shown are composite fits for n = 10–14 oocytes for WT GluN2A and n = 12 oocytes for GluN2A-E551K receptors. Insets show inward current traces for WT (black line) and E551K (blue line) receptor responses to increasing glutamate (A) (0.03, 0.1, 0.3, 1, 3, 10, and 100 μM) or glycine (B) (0.01, 0.03, 0.1, 0.3, 1, 10, and 100 μM) normalized to the current produced in maximal glutamate and glycine (100 μM each). (C–D) Concentration-response curves for glutamate (panel C) and glycine (panel D) activation of GluN1/GluN2B-A639V (open circles) and GluN1/GluN2B-G543R (open squares) compared with WT GluN1/GluN2B (black circles) receptors. Shown are composite fits for n = 24-31 oocytes for WT GluN2B, n = 12 oocytes for GluN2B-A639V, and n = 15 for GluN2B-G543R receptors. Insets show inward current traces for WT (black line), A639V (gray line), and G543R (blue line) receptor responses to increasing glutamate (C) (0.01, 0.03, 0.1, 0.3, 1, 10, and 100 μM) or glycine (D) (0.003, 0.01, 0.03, 0.1, 0.3, 3, and 100 μM) normalized to the current produced in maximal glutamate and glycine (100 μM each). Standard errors are shown when larger than the symbol size. Graphs are compiled from multiple (n=2-3) experiments with each experiment consisting of overlapping but non-identical glutamate or glycine concentrations to build the composite curves. Note that all potency shifts in variant-containing N-methyl-D-aspartate receptors were in a gain-of-function direction, and EC_{50} values were significantly different from WT controls ($P < 0.001$) by unpaired t test (2A-E551K) or one-way ANOVA and Dunnett's (2B-A639V, 2B-G543R) (statistics performed on log EC_{50}'s).

and presence of drug under maximal receptor activation by glutamate and glycine (100 μM each).

Statistical Analysis. Data are expressed as mean ± SEM, or mean ± 95% confidence interval, and the number of replicates (n) reported for each measure. One-way ANOVA with Dunnett's Multiple Comparison Test (GraphPad Prism 9.0) was used to assess significance of potential changes in the mean current in response to a single concentration of inhibitor. For potency shifts of agonists or modulators, statistical comparisons were made and 95% confidence intervals were calculated from the log IC_{50} or log EC_{50} values for comparison among conditions.

Results

GRIN Variants Selected for Rescue Pharmacology in Triheteromeric NMDARs. We selected a set of rare *GRIN* variants identified in patients with a neurologic phenotype, a de novo heterozygous genotype (Table 1), and an overall GoF designation based on electrophysiological endpoints measured in vitro by recombinant expression in *Xenopus laevis* oocytes (Supplemental Table S2; Fig. 1). We report here GoF effects for three variants reported in ClinVar (Table 1) by measuring both glutamate and glycine potency of diheteromeric variant containing NMDA receptors expressed in vitro in *Xenopus* oocytes. In this receptor context, the 2A-E551K variant (Fig. 1A,B) exhibits several-fold enhanced potency for both glutamate of 0.47 μM [0.41–0.52 μM 95% confidence interval (CI)] versus 2.9 μM (2.2–3.5 μM 95% CI) for WT 2A and glycine of 0.24 μM (0.19–0.29 μM 95% CI) versus 1.2 μM (1.0–1.4 μM 95% CI) for WT 2A EC_{50} values that were significant ($P < 0.001$, t-test performed on log EC_{50}'s). Similarly, the 2B-G543R and 2B-A639V variants (Fig. 1C,D) also exhibited several-fold enhanced potency for both glutamate of

Downloaded from jpet.aspetjournals.org at ASPET Journals on April 19, 2024

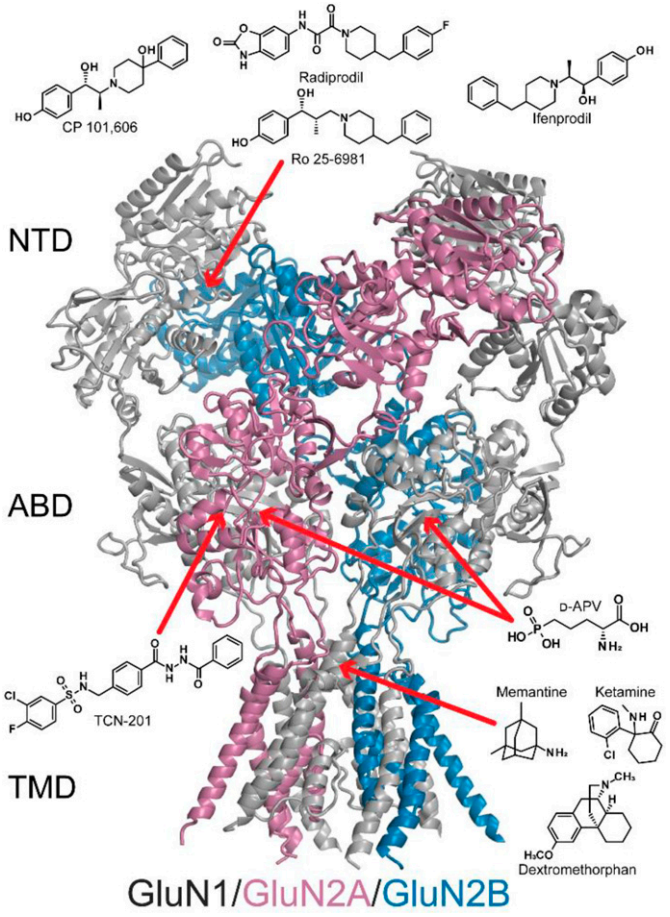

Fig. 2. Structure of noncompetitive (CP-101,606, radiprodil, Ro 25-6981, ifenprodil, TCN-201), uncompetitive (memantine, ketamine, dextromethorphan) and competitive (D-(-)-2-amino-5-phosphonopentanoic acid) inhibitors used in this study are shown, with indication of domains at which they bind on a ribbon structure of a GluN1/GluN2A/GluN2B triheteromeric receptor (PDB: 5UOW; Lü et al., 2017).

0.22 μM (0.19–0.26 μM 95% CI) for 2B-G543R and 0.28 μM (0.21–0.37 μM 95% CI) for 2B-A639V versus 1.0 μM (0.90–1.2 μM 95% CI) for WT 2B and glycine of 0.09 μM (0.08–0.12 μM 95% CI) for 2B-G543R and 0.07 μM (0.05–0.09 μM 95% CI) for 2B-A639V versus 0.33 μM (0.26–0.41 μM 95% CI) for WT 2B EC_{50} values that were significant ($P < 0.001$, one-way ANOVA, Dunnett's, performed on log EC_{50}s).

We focused on GoF variants given the availability of several NMDAR inhibitors that are either FDA-approved for use in man (memantine, ketamine, dextromethorphan), have been tested in phase 2 clinical studies (radiprodil, CP-101,606; e.g., Preskorn et al., 2008, Auvin et al., 2020), or are tool compounds that are known to be highly selective for GluN2B (ifenprodil, Ro 25-6981) or GluN2A (TCN-201; Hansen et al., 2021) diheteromeric receptors. We also evaluated a competitive antagonist at the glutamate site (D-APV) (Fig. 2). Six *GRIN2A* GoF variants were evaluated, including E551K and P552R in the pre-M1 linker region, S644G and L649V in the M3 transmembrane domain, L812M in the pre-M4 linker, and M817V in the M4 transmembrane domain (Table 1; Fig. 3). Four *GRIN2B* variants were also selected, including G543R in the pre-M1 linker region, A639V in the M3 transmembrane domain, and the M818T and A819T in the M4 transmembrane domain (Table 1; Fig. 3). All ten variant residues are located in critical receptor subunit subdomains that are intolerant to genetic variation based on absence of variants reported in the gnomAD database (v2.1.1 accessed 10-19-2021) (Fig. 3). Furthermore, these ten amino acid residues are highly conserved both phylogenetically and across the four NMDAR GluN2 subunits (GluN2A, 2B, 2C, 2D). These de novo genetic variants were identified in patients with epilepsy and/or developmental delay (Table 1). However, there is no information available about the pharmacological effects of different NMDAR inhibitors on these variants in the context of missense variant-containing triheteromeric NMDA receptors and only limited information when in the context of diheteromeric receptors (Supplemental Table S1).

To selectively express triheteromeric NMDA receptors at the cell surface, we used an expression paradigm with two engineered C-terminal peptide tags to control subunit stoichiometry within the tetrameric NMDAR, as described previously (Hansen et al., 2014; see *Methods*). An additional control with a glutamate-insensitive mutation that only produced measurable agonist-dependent currents when diheteromeric receptor "escape" from ER retention was used to verify the efficiency of the peptide tags for controlling surface expression (see Methods). The percent of escape diheteromeric currents measured were between 1 and 6% of the recorded triheteromeric response, suggesting that greater than 94% of the current was from surface triheteromeric NMDARs (Supplemental Figure S1).

We evaluated the noncompetitive GluN2A-selective inhibitor TCN-201 and noncompetitive GluN2B-selective inhibitors ifenprodil, radiprodil, Ro 25-6981, and CP-101,606 for actions on triheteromeric NMDARs containing GoF variants. We compared the effects of these subunit-selective compounds to the FDA-approved channel blockers memantine, ketamine, and dextromethorphan in addition to the competitive antagonist D-APV, none of which show any appreciable subunit-selectivity. We first established efficiency of inhibition of GluN2A- and GluN2B-selective inhibitors on triheteromeric receptors by testing saturating concentrations (e.g., 3 μM) of these compounds using two-electrode voltage clamp current recording from *Xenopus* oocytes expressing WT and variant-containing triheteromeric NMDARs. For inhibitors with appreciable activity, we evaluated the concentration-response relationship to determine IC_{50}s.

Inhibition of Triheteromeric NMDARs by a GluN2A-Selective Negative Allosteric Modulator. The GluN2A-selective inhibitor TCN-201 showed strong inhibitory effects on diheteromeric GluN1/GluN2A_{C1}/GluN2A_{C2} receptors and no inhibition on GluN1/GluN2B_{C1}/GluN2B_{C2} NMDARs, as expected (Table 2; Fig. 4A). TCN-201 also showed relatively strong inhibition on GluN1/GluN2A_{C1}/GluN2B_{C2} WT triheteromeric receptors that approached 59% (Fig. 4; Table 2), as previously reported (Hansen et al., 2014). By contrast, TCN-201 displayed weak or no inhibition on pre-M1 and M3 GluN2A GoF variants within triheteromeric receptors (E551K, P552R, S644G, L649V) with maximal inhibition ranging from 0–17%. This may in part reflect the higher potency of glycine at these variants, given that the mechanism of action of TCN-201 involves an allosteric reduction in glycine affinity (Hansen et al., 2012). TCN-201 was more effective at inhibiting pre-M4/M4 *GRIN2A* variants L812M and M817V (24–31%; Table 2), yet was still less effective than its inhibition at WT GluN1/GluN2A_{C1}/GluN2B_{C2} NMDARs (59%; Table 2).

Downloaded from jpet.aspetjournals.org at ASPET Journals on April 19, 2024

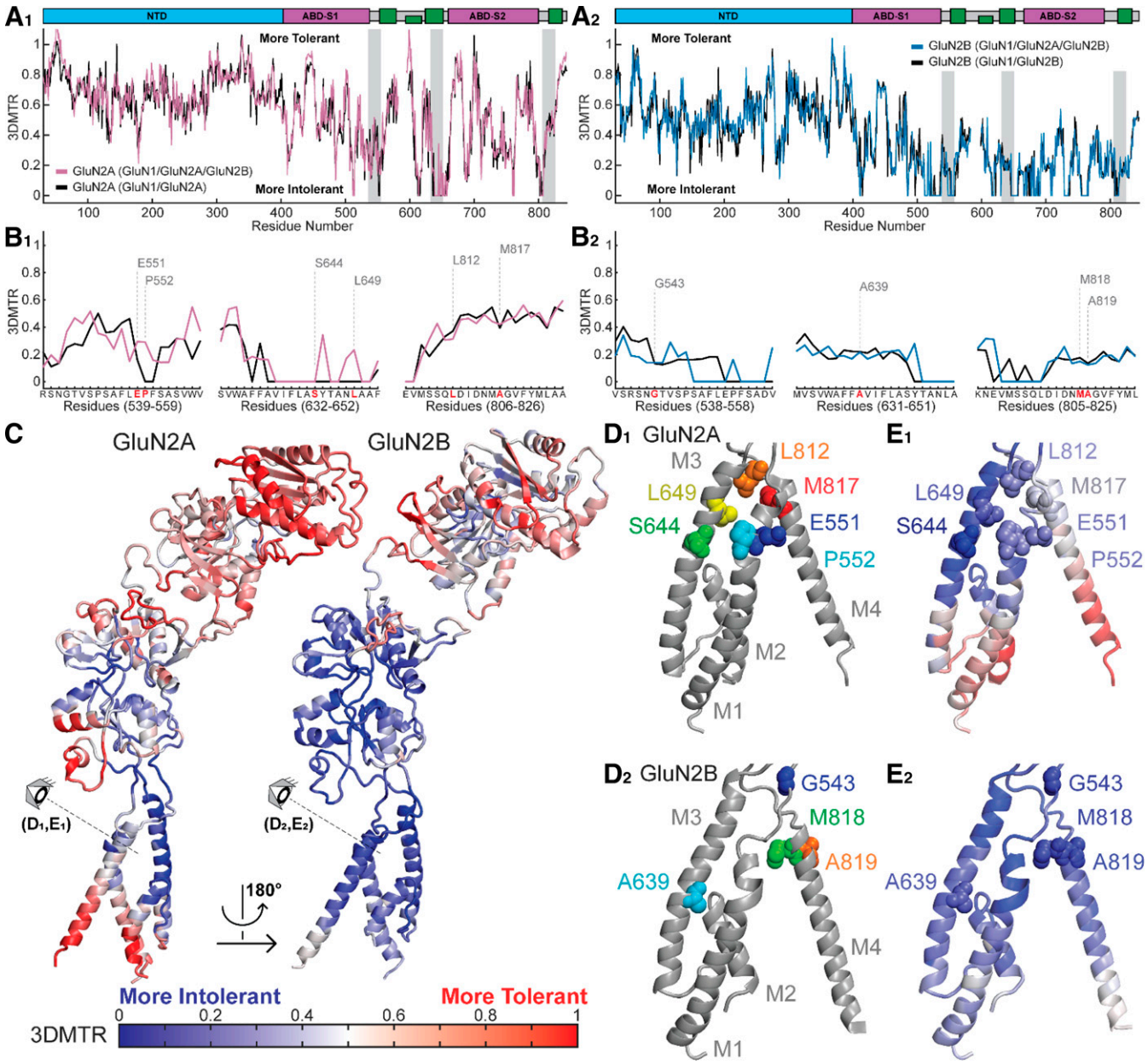

Fig. 3. Location and missense tolerance of the set of de novo variants. (A) three-dimensional missense tolerance (3DMTR) of the GluN1/GluN2A/GluN2B triheteromeric N-methyl-D-aspartate receptor from Lü et al., 2017 (PDB: 5UOW) is compared with the diheteromeric GluN1/GluN2A and GluN1/GluN2B models (A_1 shows GluN2A, A_2 shows GluN2B; Perszyk et al., 2021). (B) The 3DMTR of the de novo variants and the adjacent residues is shown (B_1 shows GluN2A, B_2 shows GluN2B); the segments shown here are depicted by the gray bands in A. (C) The individual GluN2 subunits are shown in isolation with the 3DMTR applied to each residue according to the color map shown below. (D) A closer view of the TMD highlighting the de novo variants tested in this study (E_1, GluN2A; E_2, GluN2B). (E) A closer view of the 3DMTR of the set of de novo variants tested, similar to D, using the same color map as in C.

We also evaluated the ability of TCN-201 to inhibit triheteromeric NMDARs that contained a *GRIN2B* variant. TCN-201 produced relatively strong inhibition at saturating concentrations on the *GRIN2B* pre-M1 variant G543R (46%; Table 2) but exhibited modest actions on *GRIN2B* M3 and M4 variants A639V, M818T, and A819T (6–15% inhibition; Table 2).

Because the *GRIN2B*-G543R variant showed the largest % inhibition at saturating TCN-201 concentrations, we also determined an IC_{50} for this variant by TCN-201. In a GluN1/$GluN2A_{C1}$/GluN2B-$G543R_{C2}$ triheteromeric NMDAR, the IC_{50} was 1.5 μM, which compares well with the IC_{50} of 1.2 μM at WT GluN1/$GluN2A_{C1}$/$GluN2B_{C2}$ NMDARs (Table 3, Fig. 4B).

Inhibition of Triheteromeric NMDARs by GluN2B-Selective Negative Allosteric Modulators. We next evaluated four GluN2B-selective inhibitors (ifenprodil, Ro 25-6891, radiprodil, CP-101,606) at saturating concentrations for actions on triheteromeric receptors that contained one copy of either a *GRIN2A* or *GRIN2B* variant. As reported previously, all GluN2B-selective inhibitors blocked GluN1/$GluN2B_{C1}$/$GluN2B_{C2}$ WT NMDARs with similar maximum efficacy as GluN1/GluN2B WT NMDARs (Table 2, Fig. 4C,F,G,H; Hansen et al., 2014; Mullier et al., 2017), with little effect on GluN1/$GluN2A_{C1}$/$GluN2A_{C2}$ NMDARs (Fig. 4C,F,G,H; Table 2). GluN2B-selective inhibitors have been

Downloaded from jpet.aspetjournals.org at ASPET Journals on April 19, 2024

TABLE 2
Percent inhibition of triheteromeric N-methyl-D-aspartate receptors to inhibitors at saturating concentration

Subunits	TCN-201 Inhibition %,(n)	Ifenprodil Inhibition %,(n)	Radiprodil Inhibition %,(n)	Ro 25-6981 Inhibition %,(n)	CP-101,606 Inhibition %,(n)	Memantine Inhibition %, (n)	Ketamine Inhibition %, (n)	Dextromethorphan Inhibition %, (n)
2A/2A	95 ± 1.6 (19)*	no inhibition	no inhibition	no inhibition	no inhibition	94 ± 0.73 (20)	92 ± 1.5 (12)	91 ± 1.2 (18)
2B/2B	no inhibition	85 ± 1.6 (20)*	86 ± 0.89 (16)*	89 ± 2.0 (13)*	84 ± 1.5 (16)*	97 ± 0.42 (17)	93 ± 1.1 (14)	96 ± 1.3 (14)
2A/2B	59 ± 3.7 (19)	31 ± 1.3 (20)	28 ± 2.0 (14)	27 ± 3.7 (17)	18 ± 3.1 (17)	95 ± 0.61 (21)	91 ± 0.92 (15)	93 ± 0.92 (15)
2A-E551K/2B	17 ± 3.6 (9)*	22 ± 3.0 (11)	19 ± 3.0 (12)*	30 ± 2.7 (12)	39 ± 1.8 (13)*	94 ± 1.6 (14)	89 ± 1.2 (12)	89 ± 1.9 (11)
2A-P552R/2B	6.3 ± 3.7 (14)*	46 ± 2.1 (13)*	54 ± 2.1 (12)*	44 ± 5.1 (11)*	41 ± 3.6 (14)*	95 ± 0.67 (14)	92 ± 1.1 (12)	91 ± 1.7 (10)
2A-S644G/2B	15 ± 1.9 (14)*	10 ± 2.1 (13)*	6.4 ± 2.3 (15)*	9.0 ± 5.0 (12)*	0.6 ± 0.3 (12)*	87 ± 1.5 (15)*	80 ± 1.3 (15)*	91 ± 1.3 (12)
2A-L649V/2B	2.4 ± 1.4 (11)*	7.0 ± 2.3 (12)*	5.0 ± 3.5 (11)*	4.0 ± 3.6 (12)*	2.3 ± 0.7 (11)*	95 ± 0.51 (12)	79 ± 1.3 (13)*	94 ± 0.89 (11)
2A-L812M/2B	24 ± 4.8 (12)*	14 ± 2.3 (12)*	13 ± 3.1 (12)*	10 ± 1.8 (11)*	4.4 ± 2.3 (12)*	92 ± 1.1 (12)	86 ± 1.6 (13)	84 ± 3.0 (12)*
2A-M817V/2B	31 ± 5.6 (12)*	14 ± 2.8 (14)*	6.0 ± 2.1 (11)*	2.0 ± 1.6 (12)*	1.3 ± 0.6 (11)*	90 ± 1.4 (13)	81 ± 2.1 (13)*	88 ± 2.3 (11)
2A/2B-G543R	46 ± 0.59 (10)	35 ± 3.6 (12)	33 ± 2.2 (11)	44 ± 1.8 (11)*	46 ± 1.8 (11)*	95 ± 1.0 (12)	94 ± 1.5 (11)	90 ± 1.2 (10)
2A/2B-A639V	6.3 ± 1.2 (10)*	12 ± 1.7 (12)*	5.6 ± 3.3 (11)*	6.0 ± 2.7 (11)*	7.9 ± 2.7 (12)	83 ± 3.1 (12)*	82 ± 2.3 (13)*	90 ± 0.49 (10)
2A/2B-M818T	15 ± 3.5 (10)*	43 ± 3.2 (11)*	24 ± 2.3 (10)	26 ± 4.4 (12)	27 ± 4.5 (10)	92 ± 1.5 (12)	87 ± 2.0 (12)	90 ± 2.6 (11)
2A/2B-A819T	14 ± 4.4 (9)*	41 ± 2.8 (12)*	13 ± 2.3 (11)*	13 ± 2.3 (11)*	20 ± 4.9 (10)	91 ± 2.8 (13)	87 ± 1.9 (10)	92 ± 0.79 (12)

Data are percent inhibition compared with drug-free control current responses to maximally effective concentrations of glutamate (100 μM) and glycine (100 μM) for ifenprodil, radiprodil, Ro 25-6981, CP-101,606, memantine, ketamine, and dextromethorphan determined using two-electrode voltage-clamp recordings from *Xenopus* oocytes. For TCN-201, receptor responses were evoked with 100 μM of glutamate and 3 μM of glycine. V_{HOLD} was -40 mV for all experiments. Ifenprodil, radiprodil, Ro 25-6981, CP-101,606, and TCN-201 were evaluated at 3 μM, whereas memantine and ketamine were evaluated at 100 μM, and dextromethorphan was tested at 300 μM. Data are mean ± SEM; the number of oocytes recorded is given in parentheses. *$P < 0.05$, significant compared with WT 2A/2B by one-way ANOVA with Dunnett's multiple comparison test.

reported to have reduced potency and a diminished maximal inhibition of triheteromeric GluN1/GluN2A_{C1}/GluN2B_{C2} WT NMDARs (e.g., Hatton and Paoletti, 2005; Hansen et al., 2014), and we also report diminished maximal inhibition ranging from 18–31% for four GluN2B-selective NAMs (Fig. 4C-H, Table 2).

To better understand the potential effects of the GluN2B-selective NAMs on *GRIN2A* variants that exist within triheteromeric GluN1/GluN2A_{C1}/GluN2B_{C2} NMDARs, we first measured the ability of these GluN2B-selective inhibitors to maximally inhibit triheteromeric NMDARs that contain a single copy of a *GRIN2A* variant (Fig. 3C-H; Table 2). These four inhibitors showed variable effects. No GluN2B-selective NAM was particularly effective at maximally inhibiting GluN1/GluN2A_{C1}/GluN2B_{C2} triheteromeric NMDARs that contained *GRIN2A* M3, pre-M4, or M4 variants, with 0.6–14% maximal inhibition observed at saturating concentrations for each inhibitor. However, the GluN2B NAMs were more effective at maximally reducing current responses for *GRIN2A* pre-M1 variants E551K or P552R (19–54%; Fig. 4C,E,F,G,H; Table 2).

We also tested the GluN2B-selective inhibitors on triheteromeric GluN1/GluN2A_{C1}/GluN2B_{C2} receptors that contained a single copy of a damaging *GRIN2B* variant. Here, maximal inhibition of triheteromeric receptors that contained *GRIN2B* variants G543R and M818T (24–46% inhibition) (Fig. 4C,F,G,H) was similar across the four inhibitors, whereas for the *GRIN2B* variant A819T, maximal inhibition was more variable across the four inhibitors (13–41% inhibition). All four inhibitors were only modestly effective at blocking responses of the *GRIN2B* M3 variant A639V (5.6–12% inhibition; Table 2, Fig. 4C,F,G,H).

We subsequently measured the potency of ifenprodil to inhibit five variants in the context of triheteromeric NMDARs. We selected ifenprodil as a representative GluN2B-selective inhibitor given its widespread use in the literature. In these studies, ifenprodil potency was reduced approximately 1.2- to 2.4-fold for the *GRIN2A* E551K and P552R variants, and from 3.2- to 3.6-fold for the *GRIN2B* G543R, M818T, and A819T variants when tested in the context of a triheteromeric receptor (Table 3; Fig. 4D; Supplemental Table S3), suggesting that while they retain effectiveness on inhibiting variant receptors, somewhat higher concentrations are required. For example, radiprodil reduced the current response of GluN1/GluN2A_{C1}/GluN2B_{C2} WT NMDARs with an IC_{50} of 50 nM and maximal inhibition of 29%, and inhibited GluN1/GluN2A-P552R_{C1}/GluN2B_{C2} NMDARs with an IC_{50} of 135 nM and maximal inhibition of 54% (Supplemental Figure S2).

Inhibition of Triheteromeric NMDARs by Channel Blockers. Three US Food and Drug Administration-approved NMDAR channel blockers (memantine, ketamine, dextromethorphan) were also evaluated at variant-containing triheteromeric NMDARs. All channel blockers tested inhibited both triheteromeric GluN1/GluN2A_{C1}/GluN2B_{C2} WT and variant NMDARs. We first determined the degree of inhibition by a maximally effective concentration of channel blocker (100 μM for memantine, ketamine; 300 μM for dextromethorphan). Maximally effective concentrations of memantine inhibited WT GluN1/GluN2A_{C1}/GluN2B_{C2} by 95%, triheteromeric *GRIN2A* GoF variants by 87–95%, and triheteromeric *GRIN2B* GoF variants by 83–95% (Table 2). We subsequently recorded the concentration-response curve for NMDAR channel blockers dextromethorphan, memantine, and ketamine on triheteromeric GluN1/GluN2A_{C1}/GluN2B_{C2} NMDARs harboring either GoF *GRIN2A* or *GRIN2B* variants (Fig. 5; Table 3). Triheteromeric GluN1/GluN2A_{C1}/GluN2B_{C2} NMDARs showed intermediate sensitivity to memantine (IC_{50} 3.4 μM) compared with diheteromeric GluN1/GluN2A_{C1}/GluN2A_{C2} (IC_{50} 6.4 μM) or GluN1/GluN2B_{C1}/GluN2B_{C2} (IC_{50} 2.3 μM). Ketamine similarly showed an intermediate potency at triheteromeric receptors compared with diheteromeric receptors, whereas dextromethorphan had similar potency at triheteromeric NMDARs (Table 3). This is consistent with the idea that the sites of interaction within the pore blockers are not identical between different channel blockers (e.g., LePage et al., 2005). The IC_{50} was determined for all ten GoF *GRIN2A* and *GRIN2B* variants when expressed in triheteromeric receptor contexts. Here, memantine showed similar potency for pre-M1 *GRIN2A* variants E551K and P552R when expressed in

Downloaded from jpet.aspetjournals.org at ASPET Journals on April 19, 2024

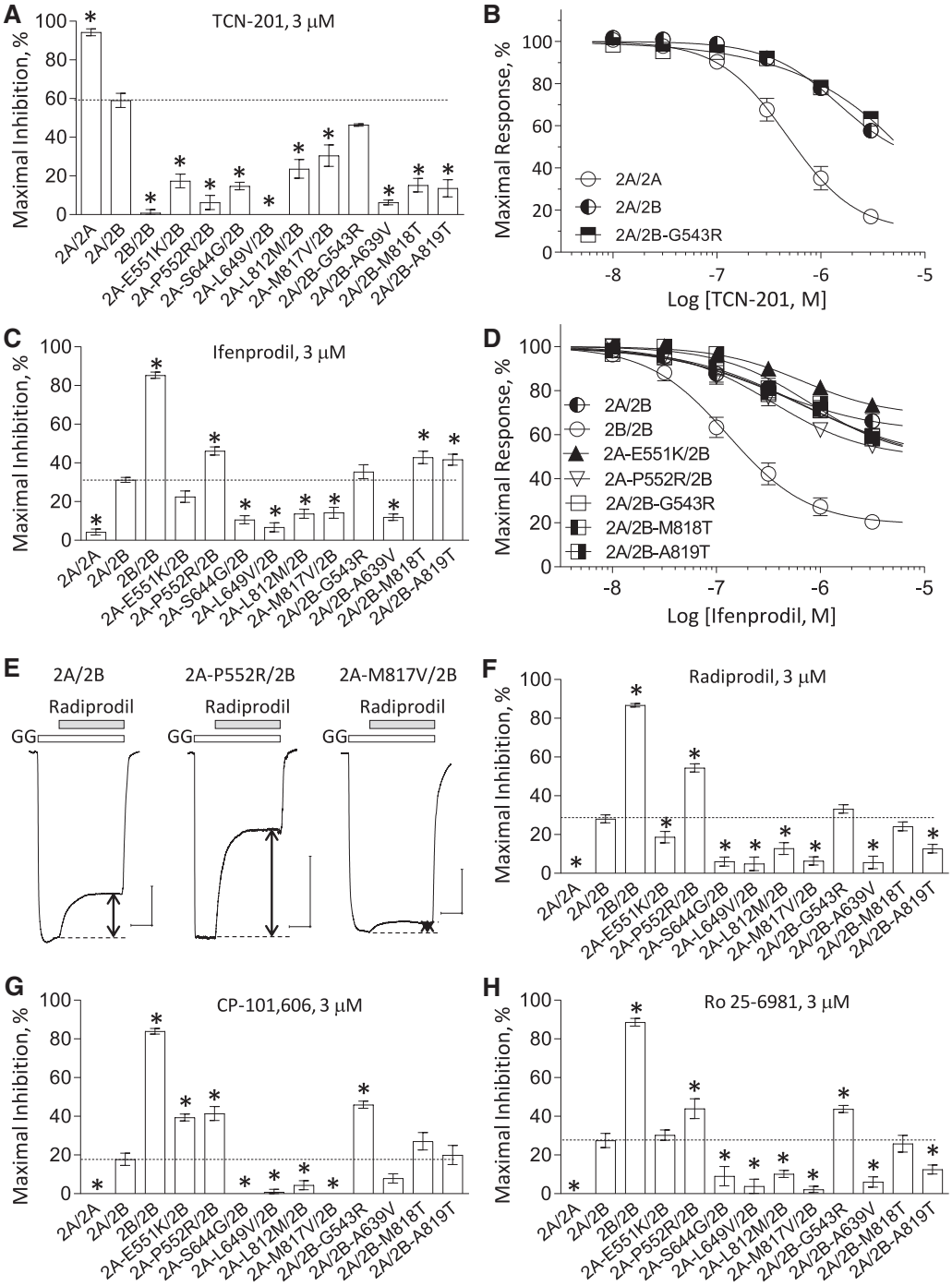

Fig. 4. Sensitivity of variant-containing triheteromeric N-methyl-D-aspartate receptors (NMDARs) to subunit-selective inhibitors. (A, C, F, G, H). A bar graph summarizes the degree of maximal inhibition produced by a maximally effective concentration (3 μM) of the indicated GluN2A- or GluN2B-selective inhibitors. *$P < 0.05$, significant compared with WT 2A/2B by one-way ANOVA with Dunnett's multiple comparison test. See Table 2 for number of oocytes. *B,D.* Concentration-response curves are shown for GluN2A- and GluN2B-selective inhibitors acting at variant-containing triheteromeric GluN1/GluN2A$_{C1}$/GluN2B$_{C2}$ NMDARs. Results shown are the Mean±S.E.M. See Table 3 for number of oocytes. While similar, the degree of maximal inhibition for TCN-201 in A and B are not identical due to different duration of drug application; longer application time (3 minutes) in the single concentration experiments with 3 μM produced somewhat stronger inhibition than 1-minute application for concentration-response experiments. *E.* Response time course for NMDAR currents recorded from oocytes show activation by glutamate and glycine (GG, 100 μM each) and effect of radiprodil (3 μM) at WT GluN1/GluN2A/GluN2B and NMDARs containing two different variants (GluN2A-P552R or GluN2A-M817V) expressed as triheteromeric GluN1/GluN2A$_{C1}$/GluN2B$_{C2}$ NMDARs. Scale bars are 1 minute and 100 nA in each panel.

GluN1/GluN2A$_{C1}$/GluN2B$_{C2}$ triheteromeric NMDARs, but a 3- to 7-fold loss in potency for inhibition of the other four *GRIN2A* variants in M3, pre-M4, and M4 domains (Fig. 5A; Table 3; Supplemental Table S3). A similar pattern was observed for ketamine and dextromethorphan, where pre-M1 variants had only modest effects on IC$_{50}$ values for these channel blockers (Fig. 5B,C; Table 3; Supplemental Table S3). We also evaluated the actions of channel blockers on the

Downloaded from jpet.aspetjournals.org at ASPET Journals on April 19, 2024

TABLE 3
Potency of inhibitors at triheteromeric N-methyl-D-aspartate receptors

Subunit	TCN-201 IC_{50}, μM (CI)(n)	Ifenprodil IC_{50}, μM (CI)(n)	Memantine IC_{50}, μM (CI)(n)	Ketamine IC_{50}, μM (CI)(n)	Dextromethorphan IC_{50}, μM (CI)(n)	D-APV IC_{50}, μM (CI)(n)
2A/2A	0.50 (0.30,0.85) (8)	_	6.4 (5.2,8.0) (13)*	6.0 (4.4,7.9) (18)	15 (11,21) (20)	0.67 (0.59,0.76) (13)
2B/2B	_	0.13 (0.10,0.16) (18)*	2.3 (1.8,2.8) (15)	2.1 (0.8,5.8) (16)*	9.8 (6.8,14) (17)	1.7 (1.3,2.1) (12)*
2A/2B	1.2 (0.9,1.7) (12)	0.27 (0.18,0.41) (19)	3.4 (2.9,4.0) (18)	4.5 (2.1,7.4) (16)	13 (10,17) (18)	0.82 (0.71,0.94) (23)
2A-E551K/2B	_	0.65 (0.43,0.98) (8)	4.4 (3.6,5.3) (12)	6.1 (4.2,11) (13)	18 (14,24) (11)	0.74 (0.50,1.1) (13)
2A-P552R/2B	_	0.32 (0.19,0.53) (11)	4.7 (4.1,5.2) (12)	7.6 (4.3,14) (13)	17 (14,21) (12)	0.89 (0.63,1.2) (17)
2A-S644G/2B	_	_	23 (18,30) (10)*	35 (24,55) (12)*	44 (35,56) (15)*	0.83 (0.66,1.0) (15)
2A-L649V/2B	_	_	9.7 (7.3,13) (12)*	16 (9.3,24) (12)*	20 (17,24) (12)	0.76 (0.47,1.2) (9)
2A-L812M/2B	_	_	11 (8.0,15) (12)*	11 (6.3,16) (13)*	46 (35,61) (12)*	0.81 (0.68,0.96) (19)
2A-M817V/2B	_	_	13 (8.2,22) (12)*	17 (13,22) (12)*	46 (32,67) (14)*	0.96 (0.76,1.2) (10)
2A/2B-G543R	1.5 (0.86,1.6) (13)	0.87 (0.50,1.5) (12)*	2.0 (1.4,2.9) (13)*	3.4 (2.1,6.1) (11)	11 (8.0,15) (11)	0.58 (0.51,0.65 (13)
2A/2B-A639V	_	_	16 (12,21) (12)*	17 (14,24) (12)*	26 (21,33) (12)*	0.76 (0.65,0.89) (11)
2A/2B-M818T	_	0.91 (0.37,2.2) (11)*	6.1 (4.9,7.5) (14)*	6.8 (4.8,11) (11)	18 (14,24) (10)	0.80 (0.71,0.91) (12)
2A/2B-A819T	_	0.96 (0.58,1.6) (9)*	13 (8.9,21) (13)*	15 (9.4,25) (10)*	41 (31,55) (12)*	0.51 (0.42,0.62) (12)

Concentration-response curves for inhibition of N-methyl-D-aspartate receptor current responses were constructed by co-application of a variable concentration of drug and maximally effective concentration of glutamate and glycine (100 μM each) for ifenprodil, memantine, ketamine, and dextromethorphan determined using two-electrode voltage-clamp recordings from *Xenopus* oocytes. For TCN-201, responses were evoked with 100 μM of glutamate and 3 μM of glycine. V_{HOLD} was -40 mV for all experiments. For D-(-)-2-amino-5-phosphonopentanoic acid concentration-response curves, responses were evoked by co-application of an EC_{50} level of glutamate for the specific triheteromeric receptor, plus maximally effective glycine (100 μM), and variable D-(-)-2-amino-5-phosphonopentanoic acid. Glutamate EC_{50} values for all variants, and concentrations used in these experiments are given in Supplemental Table S2. Data are mean, 95% confidence intervals, and the number of oocytes (n) used to generate the data are given in parentheses. *$P < 0.05$, compared with WT GluN1/GluN2A/GluN2B by one-way ANOVA with Dunnett's multiple comparison test. Statistical comparisons made using the log IC_{50} values.

four *GRIN2B* variants expressed as triheteromeric GluN1/$GluN2A_{C1}$/$GluN2B_{C2}$ NMDARs. Here, memantine and ketamine were slightly more potent at *GRIN2B* variant G543R, slightly less potent at M818T, and 3- to 5-fold less potent but still effective inhibitors of *GRIN2B* variants A639V and A819T (Fig. 5; Table 3; Supplemental Table S3). We additionally confirmed that all channel blockers still show expected voltage dependence with block at negative potentials and minimal actions at positive potentials, with the exception of GluN2A-P552R, which showed memantine block of inward and outward currents (Fig. 6A-F). These results confirm that variants did not markedly alter the voltage-dependent mechanism of these channel blockers in triheteromeric receptors harboring most variants. In addition, the representative GluN2B-selective inhibitor radiprodil produced a voltage-independent inhibition for all receptor subunit combinations tested, as expected given its binding site in the NTD, which is at considerable distance from the transmembrane potential (Fig. 6G-I).

Inhibition of Triheteromeric NMDARs by a Competitive Antagonist. Lastly, we evaluated the effect of these GoF variants on inhibition produced by a competitive antagonist that bound to the glutamate binding site on the GluN2 subunit. To determine comparable IC_{50} values for D-APV, we first determined the glutamate EC_{50} value for all ten variants (Supplemental Table S2). This allowed us to produce concentration-response curves for D-APV inhibition of NMDARs activated by appropriate EC_{50} levels of glutamate per variant. In this situation, the IC_{50} value that we determine for D-APV approximates its K_B value at each variant receptor, allowing us to determine whether the variants altered the sensitivity of the receptor to binding of D-APV. Determination of the IC_{50} values for D-APV inhibition of NMDAR responses with EC_{50}-levels of glutamate showed less than 2.1-fold variation across all variants, (Fig. 7; Table 3; Supplemental Table S3). These data are consistent with the location of the variants, which in all cases were in the transmembrane or linker regions and outside of the agonist binding domain that contains the agonist and D-APV binding site (Fig. 2).

Discussion

The mammalian brain contains a wide range of NMDA receptors of varying subunit composition. Many of these are triheteromeric receptors that contain two different GluN2 subunits (Sheng et al., 1994; Luo et al., 1997; Al-Hallaq et al., 2007; Rauner and Kohr, 2011; Tovar et al., 2013; Hansen et al., 2021). We have studied the pharmacology of triheteromeric NMDARs that contain a single copy of a *GRIN2A* or a *GRIN2B* variant identified in patients with neurologic conditions. Several important insights are apparent from the results presented here. First, we found that the prototypical GluN2A-selective inhibitor TCN-201 is capable of attenuating current for triheteromeric receptors that contain some (but not all) *GRIN2B* variants tested. Conversely, GluN2B-selective inhibitors, including ifenprodil and its analogs (CP-101,606, Ro 25-6981, radiprodil), can attenuate triheteromeric receptor responses that contain certain *GRIN2A* variants. These results suggest that if such subunit-selective inhibitors become available for clinical use in the future, their utility in the context of NMDAR variants could extend beyond their specified subunit selectivity. That is, since GluN2B-selective inhibitors are still modestly active at GluN2A- and GluN2B-containing triheteromeric NMDA receptors, they might also be considered for use against *GRIN2A* GoF variants. While this idea is raised by the results here, it will require more thorough evaluation in animal models. One animal model has shown a modest potential effect of radiprodil on a *GRIN2A* variant, S644G (Amador et al., 2020). Second, the variable actions of these inhibitors underscore the necessity of functional evaluation of drug action at variant-containing receptors prior to any consideration of clinical use, as it is presently impossible to know a priori whether a given compound will be effective. This idea is consistent with results for a number of channel blockers that have been tested against NMDAR variants and have shown a range of potencies, some lower, some higher than wild-type receptors (Supplemental Tables S2; S3; Pierson et al., 2014; Marwick et al., 2019; Amador et al., 2020; Xu et al., 2021). Third, these results support the intermediate

Downloaded from jpet.aspetjournals.org at ASPET Journals on April 19, 2024

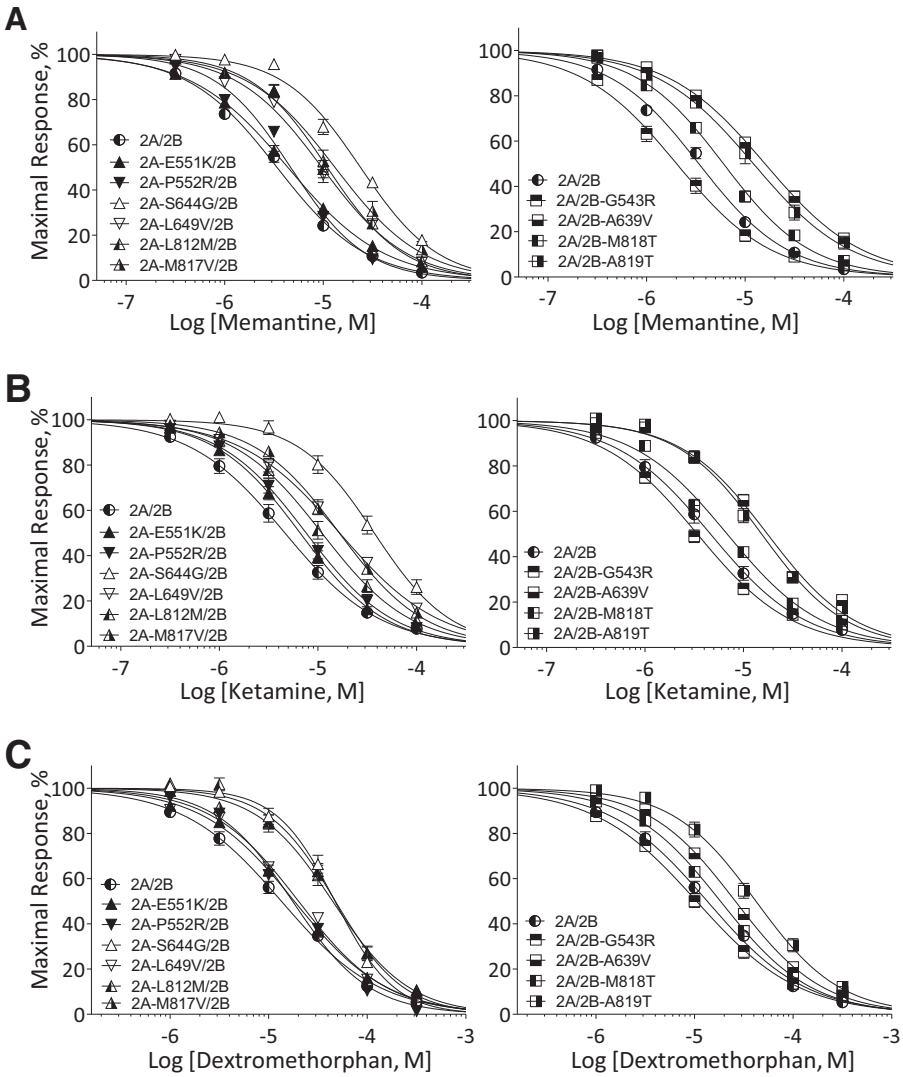

Fig. 5. Sensitivity of variant-containing triheteromeric N-methyl-D-aspartate receptors to uncompetitive channel blockers. (A–C) Concentration-response curves are shown for channel blockers acting at variant-containing triheteromeric GluN1/GluN2A$_{C1}$/GluN2B$_{C2}$ N-methyl-D-aspartate receptors. The concentration-response curves were generated at maximal concentrations of glutamate and glycine (100 μM each) at V_{HOLD}: -40 mV.

pharmacological phenotype observed for many triheteromeric receptors, which emphasizes the importance of studying these receptor subtypes in addition to diheteromeric receptors.

One important caveat to bear in mind when considering the results described here is that our method for controlling subunit stoichiometry involved both addition of the coiled-coil domains plus an ER retention signal onto GluN2 subunits downstream of the C-terminal. In addition, we replaced the GluN2B C-terminal with that for GluN2A. While the wild-type GluN2B C-terminal may be necessary for some aspects of inhibition by negative allosteric modulators, such as radiprodil that binds to the NTD, several observations suggest the data we obtained here is representative of that found for wild type triheteromeric receptors. For example, deletion of the C-terminal tails for both GluN2A and GluN2B prior to addition of coiled-coil domains yields the same results in terms of the actions of ifenprodil (Stroebel et al., 2014). Furthermore, use of a different strategy to inhibit diheteromeric receptors that does not alter the C-terminal also yields the same results for ifenprodil inhibition of triheteromeric receptors (Hatton and Paoletti, 2005), suggesting the data we obtain is representative of unmodified triheteromeric GluN1/GluN2A/GluN2B receptors. We also note that ifenprodil showed similar pharmacological properties at both wild-type GluN1/GluN2B receptors as receptors that contained our modified C-termini, GluN1/GluN2B$_{C1}$/GluN2B$_{C2}$ (Hansen et al., 2014).

An interesting result that emerged from the sensitivity of variants within triheteromeric receptors was the manner in which subunit-selective inhibitors showed activity for variants in some but not other regions of the protein. This suggests potential downstream actions of the allosteric modulators, in that variants within specific domains that are downstream of modulator binding may interrupt the activity of that modulator, rendering the inhibitor less effective. For example, *GRIN2A* pre-M1 variants were permissive for inhibition by GluN2B-selective inhibitors, but *GRIN2A* M3/Pre-M4/M4 variants were not. One hypothesis raised from this observation is that the actions of GluN2B inhibition impact molecular motions involving M3 and M4 transmembrane elements that are required for inhibition, such that variants in these regions interrupt actions of the GluN2B allosteric inhibitors by interfering with downstream conformational changes. However, this may be a special case of the triheteromeric context, perhaps due to the NTD-ABD cross-over which occurs in NMDA

Downloaded from jpet.aspetjournals.org at ASPET Journals on April 19, 2024

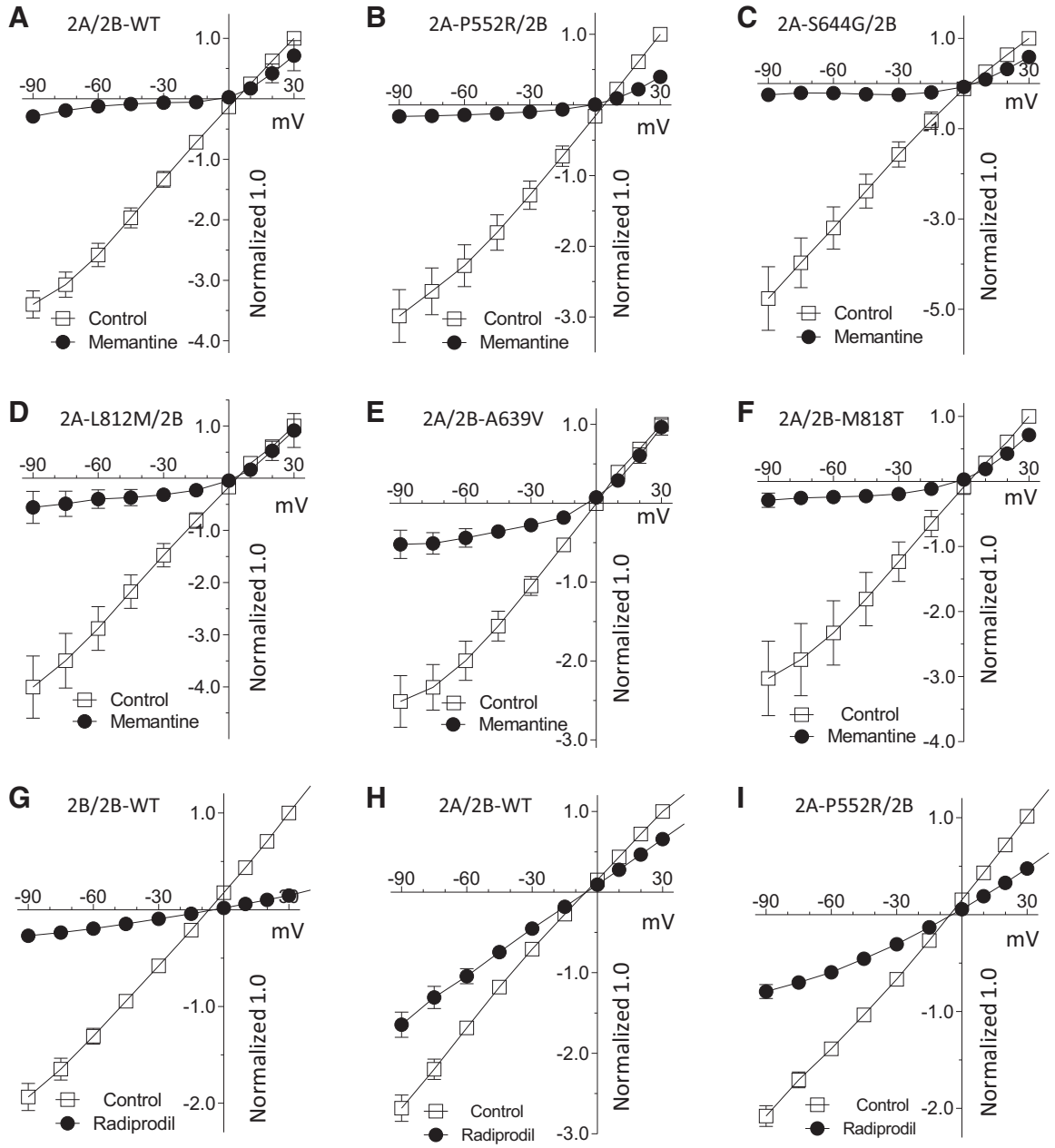

Fig. 6. Voltage-dependent inhibition of variant-containing triheteromeric N-methyl-D-aspartate receptors by memantine but not radiprodil. (A–F). The current-voltage relationship is shown for memantine (dark circles) inhibition of variant containing triheteromeric GluN1/GluN2A$_{C1}$/GluN2B$_{C2}$ N-methyl-D-aspartate receptors. The amplitude of NMDA receptor responses to maximal glutamate and glycine alone (100 μM each, open squares) recorded at different voltages are superimposed on the amplitude of responses to maximal glutamate and glycine in the presence of memantine (100 μM, filled circles). (G–I) The current-voltage relationship reveals lack of voltage dependence to inhibition of variant containing triheteromeric GluN1/GluN2A$_{C1}$/GluN2B$_{C2}$ N-methyl-D-aspartate receptors by 3 μM radiprodil (black circles) superimposed on the amplitude of responses to maximal glutamate and glycine alone (control, open squares). For all curves, current was normalized to drug-free response at +30 mV.

receptors. Thus, the mechanistic pathway connecting the NTD, agonist binding, and channel gating may not necessarily run through the GluN2B subunit alone and may be influenced by the alternate GluN2 subunit in the triheteromer context. For some variants, either in GluN2A or GluN2B, the available therapeutic options may be more broad given the triheteromeric receptor is the primary NMDA receptor subtype found in several key brain regions.

While these data provide a useful perspective on potential means to rectify aberrant NMDAR activity, it will be important and informative to evaluate drug actions at different time points during development in animal models harboring different variant NMDAR subunits to further guide precision medicine.

Acknowledgment

The authors thank Rebecca Bui, Courtney Ning, and Vincent Peterson for technical assistance in DNA preparation and oocyte injections and Jing Zhang and Phuong Le for excellent technical assistance.

Downloaded from jpet.aspetjournals.org at ASPET Journals on April 19, 2024

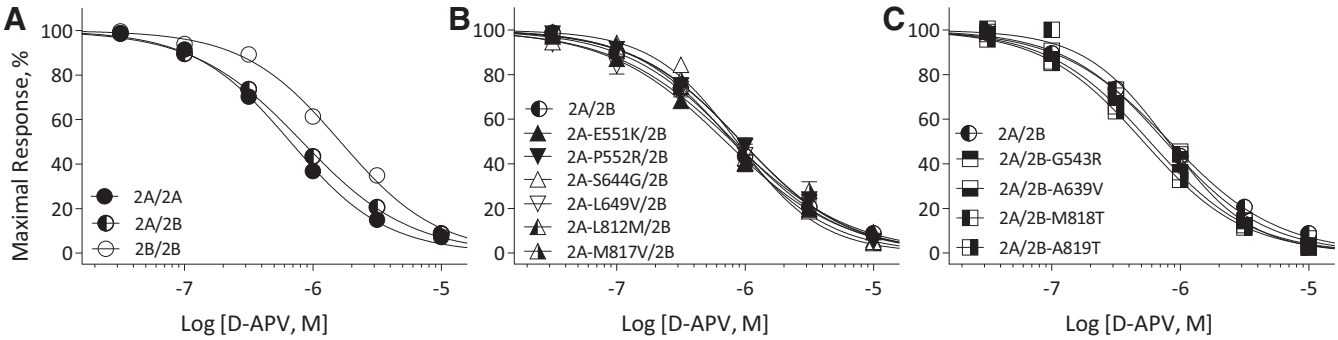

Fig. 7. Concentration-response curves for D-APV acting at wild-type (A) and variant-containing triheteromeric GluN1/GluN2A$_{C1}$/GluN2B$_{C2}$ N-methyl-D-aspartate receptors B–C. The D-APV concentration-response curve was generated at receptors activated by EC_{50} concentrations of glutamate (see Supplemental Table S2) and a maximally effective concentration of glycine (100 μM) at V_{HOLD}: -40 mV.

Authorship Contributions:

Participated in research design: Han, Yuan, Traynelis, Myers.

Conducted experiments: Han, Allen, Shaulsky, Myers, Kim.

Performed data analysis: Han, Yuan, Allen, Perszyk, Kim, Traynelis, Myers.

Wrote or contributed to the writing of the manuscript: Han, Yuan, Allen, Kim, Perszyk, Traynelis, Myers.

References

Al-Hallaq RA, Conrads TP, Veenstra TD, and Wenthold RJ (2007) NMDA di-heteromeric receptor populations and associated proteins in rat hippocampus. *J Neurosci* **27**:8334–8343.

Amador A, Bostick CD, Olson H, Peters J, Camp CR, Krizay D, Chen W, Han W, Tang W, Kanber A et al. (2020) Modelling and treating GRIN2A developmental and epileptic encephalopathy in mice. *Brain* **143**:2039–2057.

Auvin S, Dozières-Puyravel B, Avbersek A, Sciberras D, Collier J, Leclercq K, Mares P, Kaminski RM, and Muglia P (2020) Radiprodil, a NR2B negative allosteric modulator, from bench to bedside in infantile spasm syndrome. *Ann Clin Transl Neurol* **7**:343–352.

Benke TA, Park K, Krey I, Camp CR, Song R, Ramsey AJ, Yuan H, Traynelis SF, and Lemke J (2021) Clinical and therapeutic significance of genetic variation in the GRIN gene family encoding NMDARs. *Neuropharmacology* **199**:108805 10.1016/j.neuropharm.2021.108805.

Bettini E, Sava A, Griffante C, Carignani C, Buson A, Capelli AM, Negri M, Andreetta F, Senar-Sancho SA, Guiral L et al. (2010) Identification and characterization of novel NMDA receptor antagonists selective for NR2A- over NR2B-containing receptors. *J Pharmacol Exp Ther* **335**:636–644.

Bhattacharya S, Khatri A, Swanger SA, DiRaddo JO, Yi F, Hansen KB, Yuan H, and Traynelis SF (2018) Triheteromeric GluN1/GluN2A/GluN2C NMDARs with Unique Single-channel Properties are the Dominant Receptor Population in Cerebellar Granule Cells. *Neuron* **99**:315–328.e5.

Burnashev N and Szepetowski P (2015) NMDA receptor subunit mutations in neurodevelopmental disorders. *Curr Opin Pharmacol* **20**:73–82.

Chen W, Tankovic A, Burger PB, Kusumoto H, Traynelis SF, and Yuan H (2017) Functional Evaluation of a De Novo GRIN2A Mutation Identified in a Patient with Profound Global Developmental Delay and Refractory Epilepsy. *Mol Pharmacol* **91**:317–330.

de Ligt J, Willemsen MH, van Bon BWM, Kleefstra T, Yntema HG, Kroes T, Vultovan Silfhout AT, Koolen DA, de Vries P, Gilissen C et al. (2012) Diagnostic exome sequencing in persons with severe intellectual disability. *N Engl J Med* **367**:1921–1929.

Hansen KB, Wollmuth LP, Bowie D, Furukawa H, Menniti FS, Sobolevsky AI, Swanson GT, Swanger SA, Greger IH, Nakagawa T et al. (2021) Structure, Function, and Pharmacology of Glutamate Receptor Ion Channels. *Pharmacol Rev* **73**:298–487.

Hansen KB, Ogden KK, and Traynelis SF (2012) Subunit-selective allosteric inhibition of glycine binding to NMDA receptors. *J Neurosci* **32**):6197–6208.

Hansen KB, Ogden KK, Yuan H, and Traynelis SF (2014) Distinct functional and pharmacological properties of triheteromeric GluN1/GluN2A/GluN2B NMDA receptors. *Neuron* **81**:1084–1096.

Hatton CJ and Paoletti P (2005) Modulation of triheteromeric NMDA receptors by N-terminal domain ligands. *Neuron* **46**:261–274.

Helbig KL, Farwell Hagman KD, Shinde DN, Mroske C, Powis Z, Li S, Tang S, and Helbig I (2016) Diagnostic exome sequencing provides a molecular diagnosis for a significant proportion of patients with epilepsy. *Genet Med* **18**:898–905.

Hu C, Chen W, Myers SJ, Yuan H, and Traynelis SF (2016) Human GRIN2B variants in neurodevelopmental disorders. *J Pharmacol Sci* **132**:115–121.

Jackson MR, Nilsson T, and Peterson PA (1990) Identification of a consensus motif for retention of transmembrane proteins in the endoplasmic reticulum. *EMBO J* **9**:3153–3162.

Jackson MR, Nilsson T, and Peterson PA (1993) Retrieval of transmembrane proteins to the endoplasmic reticulum. *J Cell Biol* **121**:317–333.

Lau CG and Zukin RS (2007) NMDA receptor trafficking in synaptic plasticity and neuropsychiatric disorders. *Nat Rev Neurosci* **8**:413–426.

LePage KT, Ishmael JE, Low CM, Traynelis SF, and Murray TF (2005) Differential binding properties of [3H]dextrorphan and [3H]MK-801 in heterologously expressed NMDA receptors. *Neuropharmacology* **49**:1–16.

Li D, Yuan H, Ortiz-Gonzalez XR, Marsh ED, Tian L, McCormick EM, Kosobucki GJ, Chen W, Schulien AJ, Chiavacci R et al. (2016) GRIN2D Recurrent De Novo Dominant Mutation Causes a Severe Epileptic Encephalopathy Treatable with NMDA Receptor Channel Blockers. *Am J Hum Genet* **99**:802–816.

Lü W, Du J, Goehring A, and Gouaux E (2017) Cryo-EM structures of the triheteromeric NMDA receptor and its allosteric modulation. *Science* **355**:6331.

Luo J, Wang Y, Yasuda RP, Dunah AW, and Wolfe BB (1997) The majority of N-methyl-D-aspartate receptor complexes in adult rat cerebral cortex contain at least three different subunits (NR1/NR2A/NR2B). *Mol Pharmacol* **51**:79–86.

MacDermott AB, Mayer ML, Westbrook GL, Smith SJ, and Barker JL (1986) NMDA-receptor activation increases cytoplasmic calcium concentration in cultured spinal cord neurones. *Nature* **321**:519–522.

Marwick KFM, Skehel PA, Hardingham GE, and Wyllie DJA (2019) The human NMDA receptor GluN2A^{N615K} variant influences channel blocker potency. *Pharmacol Res Perspect* **7**:e00495.

Mayer ML, Westbrook GL, and Guthrie PB (1984) Voltage-dependent block by Mg2+ of NMDA responses in spinal cord neurones. *Nature* **309**:261–263.

Mony L, Kew JN, Gunthorpe MJ, and Paoletti P (2009) Allosteric modulators of NR2B-containing NMDA receptors: molecular mechanisms and therapeutic potential. *Br J Pharmacol* **157**:1301–1317.

Mullier B, Wolff C, Sands ZA, Ghisdal P, Muglia P, Kaminski RM, and André VM (2017) GRIN2B gain of function mutations are sensitive to radiprodil, a negative allosteric modulator of GluN2B-containing NMDA receptors. *Neuropharmacology* **123**:322–331.

Myers SJ, Yuan H, Kang JQ, Tan FCK, Traynelis SF, and Low CM(2019) Distinct roles of GRIN2A and GRIN2B variants in neurological conditions. *F1000Res* **8**:F1000 Faculty Rev-1940. doi: 10.12688/f1000research.18949.1.

Nowak L, Bregestovski P, Ascher P, Herbet A, and Prochiantz A (1984) Magnesium gates glutamate-activated channels in mouse central neurones. *Nature* **307**: 462–465.

Ogden KK, Chen W, Swanger SA, McDaniel MJ, Fan LZ, Hu C, Tankovic A, Kusumoto H, Kosobucki GJ, Schulien AJ et al. (2017) Molecular Mechanism of Disease-associated Mutations in the Pre-M1 Helix of NMDA Receptors and Potential Rescue Pharmacology. *PLoS Genet* **13**:e1006536 10.1371/journal.pgen.1006536.

Paoletti P, Bellone C, and Zhou Q (2013) NMDA receptor subunit diversity: impact on receptor properties, synaptic plasticity and disease. *Nat Rev Neurosci* **14**:383–400.

Perszyk RE, Myers SJ, Yuan H, Gibb AJ, Furukawa H, Sobolevsky AI, and Traynelis SF (2020) Hodgkin-Huxley-Katz Prize Lecture: Genetic and pharmacological control of glutamate receptor channel through a highly conserved gating motif. *J Physiol* **598**:3071–3083.

Perszyk RE, Kristensen AS, Lyuboslavsky P, and Traynelis SF (2021) Three-dimensional missense tolerance ratio analysis. *Genome Res* **31**:1447–1461.

Pierson TM, Yuan H, Marsh ED, Fuentes-Fajardo K, Adams DR, Markello T, Golas G, Simeonov DR, Holloman C, Tankovic A et al.; PhD for the NISC Comparative Sequencing Program (2014) *GRIN2A* mutation and early-onset epileptic encephalopathy: personalized therapy with memantine. *Ann Clin Transl Neurol* **1**:190–198.

Platzer K, Yuan H, Schütz H, Winschel A, Chen W, Hu C, Kusumoto H, Heyne HO, Helbig KL, Tang S et al. (2017) *GRIN2B* encephalopathy: novel findings on phenotype, variant clustering, functional consequences and treatment aspects. *J Med Genet* **54**:460–470.

Preskorn SH, Baker B, Kolluri S, Menniti FS, Krams M, and Landen JW (2008) An innovative design to establish proof of concept of the antidepressant effects of the NR2B subunit selective N-methyl-D-aspartate antagonist, CP-101,606, in patients with treatment-refractory major depressive disorder. *J Clin Psychopharmacol* **28**:631–637.

Rauner C and Köhr G (2011) Triheteromeric NR1/NR2A/NR2B receptors constitute the major N-methyl-D-aspartate receptor population in adult hippocampal synapses. *J Biol Chem* **286**:7558–7566.

Downloaded from jpet.aspetjournals.org at ASPET Journals on April 19, 2024

Sheng M, Cummings J, Roldan LA, Jan YN, and Jan LY (1994) Changing subunit composition of heteromeric NMDA receptors during development of rat cortex. *Nature* **368**:144–147.

Strehlow V, Heyne HO, Vlaskamp DRM, Marwick KFM, Rudolf G, de Bellescize J, Biskup S, Brilstra EH, Brouwer OF, Callenbach PMC et al.; GRIN2A study group (2019) GRIN2A-related disorders: genotype and functional consequence predict phenotype. *Brain* **142**:80–92.

Stroebel D, Carvalho S, Grand T, Zhu S, and Paoletti P (2014) Controlling NMDA receptor subunit composition using ectopic retention signals. *J Neurosci* **34**: 16630–16636.

Strong KL, Epplin MP, Ogden KK, Burger PB, Kaiser TM, Wilding TJ, Kusumoto H, Camp CR, Shaulsky G, Bhattacharya S et al. (2021) Distinct GluN1 and GluN2 structural determinants for subunit-selective positive allosteric modulation of N-Methyl-d-aspartate receptors. *ACS Chem Neurosci* **12**:79–98.

Swanger SA, Chen W, Wells G, Burger PB, Tankovic A, Bhattacharya S, Strong KL, Hu C, Kusumoto H, Zhang J et al. (2016) Mechanistic Insight into NMDA Receptor Dysregulation by Rare Variants in the GluN2A and GluN2B Agonist Binding Domains. *Am J Hum Genet* **99**:1261–1280.

Tovar KR, McGinley MJ, and Westbrook GL (2013) Triheteromeric NMDA receptors at hippocampal synapses. *J Neurosci* **33**:9150–9160.

Traynelis SF, Wollmuth LP, McBain CJ, Menniti FS, Vance KM, Ogden KK, Hansen KB, Yuan H, Myers SJ, and Dingledine R (2010) Glutamate receptor ion channels: structure, regulation, and function. *Pharmacol Rev* **62**:405–496.

XiangWei W, Jiang Y, and Yuan H (2018) De Novo Mutations and Rare Variants Occurring in NMDA Receptors. *Curr Opin Physiol* **2**:27–35.

XiangWei W, Kannan V, Xu Y, Kosobucki GJ, Schulien AJ, Kusumoto H, Moufawad El Achkar C, Bhattacharya S, Lesca G, Nguyen S et al. (2019) Heterogeneous clinical and functional features of GRIN2D-related developmental and epileptic encephalopathy. *Brain* **142**:3009–3027.

Xu Y, Song R, Chen W, Strong K, Shrey D, Gedela S, Traynelis SF, Zhang G, and Yuan H (2021) Recurrent seizure-related GRIN1 variant: Molecular mechanism and targeted therapy. *Ann Clin Transl Neurol* **8**:1480–1494.

Yi F, Bhattacharya S, Thompson CM, Traynelis SF, and Hansen KB (2019) Functional and pharmacological properties of triheteromeric GluN1/2B/2D NMDA receptors. *J Physiol* **597**:5495–5514.

Yuan H, Hansen KB, Zhang J, Pierson TM, Markello TC, Fajardo KV, Holloman CM, Golas G, Adams DR, Boerkoel CF et al. (2014) Functional analysis of a de novo GRIN2A missense mutation associated with early-onset epileptic encephalopathy. *Nat Commun* **5**:3251 10.1038/ncomms4251.

Yuan H, Low CM, Moody OA, Jenkins A, and Traynelis SF (2015) Ionotropic GABA and Glutamate Receptor Mutations and Human Neurologic Diseases. *Mol Pharmacol* **88**:203–217.

Zerangue N, Malan MJ, Fried SR, Dazin PF, Jan YN, Jan LY, and Schwappach B (2001) Analysis of endoplasmic reticulum trafficking signals by combinatorial screening in mammalian cells. *Proc Natl Acad Sci USA* **98**:2431–2436.

Address correspondence to: Scott J. Myers, Rollins Res Center, 1510 Clifton Road, Atlanta, GA 30322. E-mail: smyer01@emory.edu

Downloaded from jpet.aspetjournals.org at ASPET Journals on April 19, 2024

Supplemental Information

Opportunities for precision treatment of *GRIN2A* and *GRIN2B* gain of function variants in triheteromeric NMDA receptors

Wei Han[1,2,a], Hongjie Yuan[1,2], James P. Allen[1,2], Sukhan Kim[1,2], Gil H. Shaulsky[1,2], Riley E. Perszyk[1], Stephen F. Traynelis[1,2], and Scott J. Myers[1,2]

[1] Department of Pharmacology and Chemical Biology, [2] Center for Functional Evaluation of Rare Variants (CFERV), Emory University School of Medicine, Atlanta, Georgia, USA

[a] Current address: Department of Neurology, Children's Hospital of Chongqing Medical University, Chongqing, China

CORRESPONDING AUTHOR:
Scott J. Myers
Department of Pharmacology and Chemical Biology
Emory University School of Medicine
1510 Clifton Road, NE
Atlanta, GA 30322
Tel: 404-727-0357
E-mail: smyer01@emory.edu

SUPPLEMENTAL MATERIAL
Tables: 3
Figures: 2

RUNNING TITLE: Rescue pharmacology on disease-related *GRIN* variants

Supplemental Table S1: Inhibitor IC_{50}'s at variant diheteromeric NMDARs

Gene	Variant	TCN-201 IC_{50} (μM)	Ifenprodil IC_{50} (μM)	Radiprodil IC_{50} (μM)	Memantine IC_{50} (μM)	Ketamine IC_{50} (μM)	Dextromethorphan IC_{50} (μM)	Amantadine IC_{50} (μM)	Reference
This study									
GRIN2A	**Wild type**	0.18 – 0.30	--	--	4.2 – 5.3	4.7 – 8.4	8.5 – 18	110 – 157	Pierson et al., 2014 Swanger et al., 2016 Chen et al., 2017 Ogden et al., 2017 Amador et al., 2020 Xu et al., 2021
GRIN2A	**p.E551K**	--	--	--	--	--	--	--	*this study*
GRIN2A	**p.P552R**	>10	--	--	3.7	1.3	15	86	Ogden et al., 2017
GRIN2A	**p.S644G**	--	--	--	24	--	25	--	Amador et al., 2020
GRIN2A	**p.L649V**	--	--	--	--	--	--	--	*this study*
GRIN2A	**p.L812M**	--	--	--	12	--	33	113	Pierson et al., 2014
GRIN2A	**p.M817V**	2.7	--		29	43	23	295	Chen et al., 2017
GRIN2B	**Wild type**	--	--	0.17	0.52 – 3.0	4.3	9.1	48	Swanger et al., 2016 Platzer et al., 2017 Mullier et al., 2017 Xu et al., 2021
GRIN2B	**p.G543R**	--	--	--	--	--	--	--	*this study*
GRIN2B	**p.A639V**	--	--	--	--	--	--	--	*this study*
GRIN2B	**p.M818T**	--	--	--	3.0	--	--	--	Platzer et al., 2017
GRIN2B	**p.A819T**	--	--	--	5.0	--	--	--	Platzer et al., 2017
Other studies									
GRIN1	**p.M641I / 2A**	0.22	--	--	1.3	0.93	0.42	14	Xu et al., 2021
GRIN1	**p.M641I / 2B**	--	--	--	0.84	0.63	1.2	7.3	Xu et al., 2021
GRIN2A	**p.N615K**	--	--	--	43	--	9.0	458	Pierson et al., 2014
GRIN2A	**p.K669N**	--	--	--	4.6	--	--	--	Swanger et al., 2016
GRIN2B	**p.R540H**	--	--	0.15	0.60	--	--	--	Mullier et al., 2017
GRIN2B	**p.G611V**	--	--	--	1.0	--	--	--	Platzer et al., 2017
GRIN2B	**p.N615I**	--	--	0.11	0.30 – 0.44	--	--	--	Mullier et al., 2017 Platzer et al., 2017
GRIN2B	**p.V618G**	--	--	0.14	16 -17	--	--	--	Mullier et al., 2017 Platzer et al., 2017
GRIN2B	**p.R696H**	--	--	--	2.1	--	--	--	Swanger et al., 2016
GRIN2B	**p.S810R**	--	--	--	4.3	--	--	--	Platzer et al., 2017
GRIN2D	**Wild type**	--	--	--	0.57 – 2.5	2.2 – 4.5	4.0 – 5.1	34	Li et al., 2016 XiangWei et al., 2019
GRIN2D	**p.V667I**	--	--	--	4.0	8.1	13	189	Li et al., 2016
GRIN2D	**p.L670F**	--	--	--	>150	>2000	>300	--	XiangWei et al., 2019
GRIN2D	**p.A675T**	--	--	--	11	25	10	--	XiangWei et al., 2019
GRIN2D	**p.A678D**	--	--	--	5.8	5.1	6.8	--	XiangWei et al., 2019

Data are IC_{50} values determined from heterologous in vitro expression systems in the indicated reference. *GRIN1* p.M641I variant was co-expressed with wild type GluN2A and GluN2B, respectively.

Supplemental Table S2

Diheteromeric receptors	Glu EC_{50}, μM (CI)(n)	Source	Triheteromeric receptors	Glu EC_{50}, μM (CI)(n)	Source	Concentration Used (μM)*
2A	3.5	Yuan et al., 2014	**2A/2A**	4.3 (3.5,5.2) (7)	This study	3.0
2B	1.5	Platzer et al., 2017	**2B/2B**	1.3 (1.1,1.5) (6)	This study	1.0
—	—	—	**2A/2B**	2.2 (2.1,2.4) (9)	This study	2.5
2A-E551K	0.47 (0.41,0.52) (12)	This study	**2A-E551K/2B**	0.70 (0.31,1.6) (4)	This study	0.7
2A-P552R	0.37	Ogden et al., 2017	**2A-P552R/2B**	0.56 (0.47,0.67) (6)	This study	0.5
2A-S644G	0.18	Amador et al 2020	**2A-S644G/2B**	0.49 (0.45,0.53) (6)	This study	0.5
2A-L649V	0.05	This study	**2A-L649V/2B**	0.36 (0.24,0.53) (6)	This study	0.4
2A-L812M	0.41	Yuan et al., 2014	**2A-L812M/2B**	0.84 (0.77,0.93) (7)	This study	0.8
2A-M817V	0.39	Chen et al., 2017	**2A-M817V/2B**	0.75 (0.70,0.80) (6)	This study	0.8
2B-G543R	0.22 (0.19,0.26) (15)	This study	**2A/2B-G543R**	1.9 (1.6,2.4) (4)	This study	2.0
2B-A639V	0.28 (0.21,0.37) (12)	This study	**2A/2B-A639V**	0.58 (0.55,0.62) (3)	This study	0.6
2B-M818T	0.37	Platzer et al., 2017	**2A/2B-M818T**	0.96 (0.66,1.4) (4)	This study	1.0
2B-A819T	0.58	Platzer et al., 2017	**2A/2B-A819T**	0.71 (0.53,0.95) (5)	This study	0.7

Data generated in this study are mean and 95% confidence intervals (CI) of EC_{50} values determined from glutamate concentration-response curves recorded at -40 mV from *Xenopus* oocytes expressing the indicated diheteromeric or triheteromeric NMDA receptors. Variable concentrations of glutamate were co-applied with 100 μM glycine. The 95% confidence intervals derived from log EC_{50} values (CI) and the number of oocytes is indicated in parentheses. *Concentrations of glutamate used to determine IC_{50} values for D-APV in dose-inhibition studies reported in Figure 7 and Table 3. If no CI or n value reported see the study source listed.

Supplemental Table S3

Inhibitor IC_{50} ratios of *GRIN* variants compared to WT 2A/2B triheteromer receptors (Variant IC_{50}/WT IC_{50})

Triheteromeric receptor	TCN-201	Ifenprodil	Memantine	Ketamine	Dextro-methorphan	D-APV
2A/2A	0.4	-	1.9	1.3	1.2	0.8
2B/2B	-	0.5	0.7	0.5	0.8	2.1
2A/2B	1.0	1.0	1.0	1.0	1.0	1.0
2A-E551K/2B	-	2.4	1.3	1.4	1.4	0.9
2A-P552R/2B	-	1.2	1.4	1.7	1.3	1.1
2A-S644G2B	-	-	6.8	7.8	3.4	1.0
2A-L649V/2B	-	-	2.9	3.6	1.5	0.9
2A-L812M/2B	-	-	3.2	2.4	3.5	1.0
2A-M817V/2B	-	-	3.8	3.8	3.5	1.2
2A/2B-G543R	1.3	3.2	0.6	0.8	0.8	0.7
2A/2B-A639V	-	-	4.7	3.8	2.0	0.9
2A/2B-M818T	-	3.4	1.8	1.5	1.4	1.0
2A/2B-A819T	-	3.6	3.8	3.3	3.2	0.6

The IC_{50} values for inhibitors at the *GRIN* variant-containing NMDA triheteromer was divided by the IC_{50} at 2A/2B WT triheteromer receptors to determine a dose ratio for equal inhibition of the *GRIN* variant containing receptor. See Table 3 for IC_{50} values.

Supplemental Figure S1

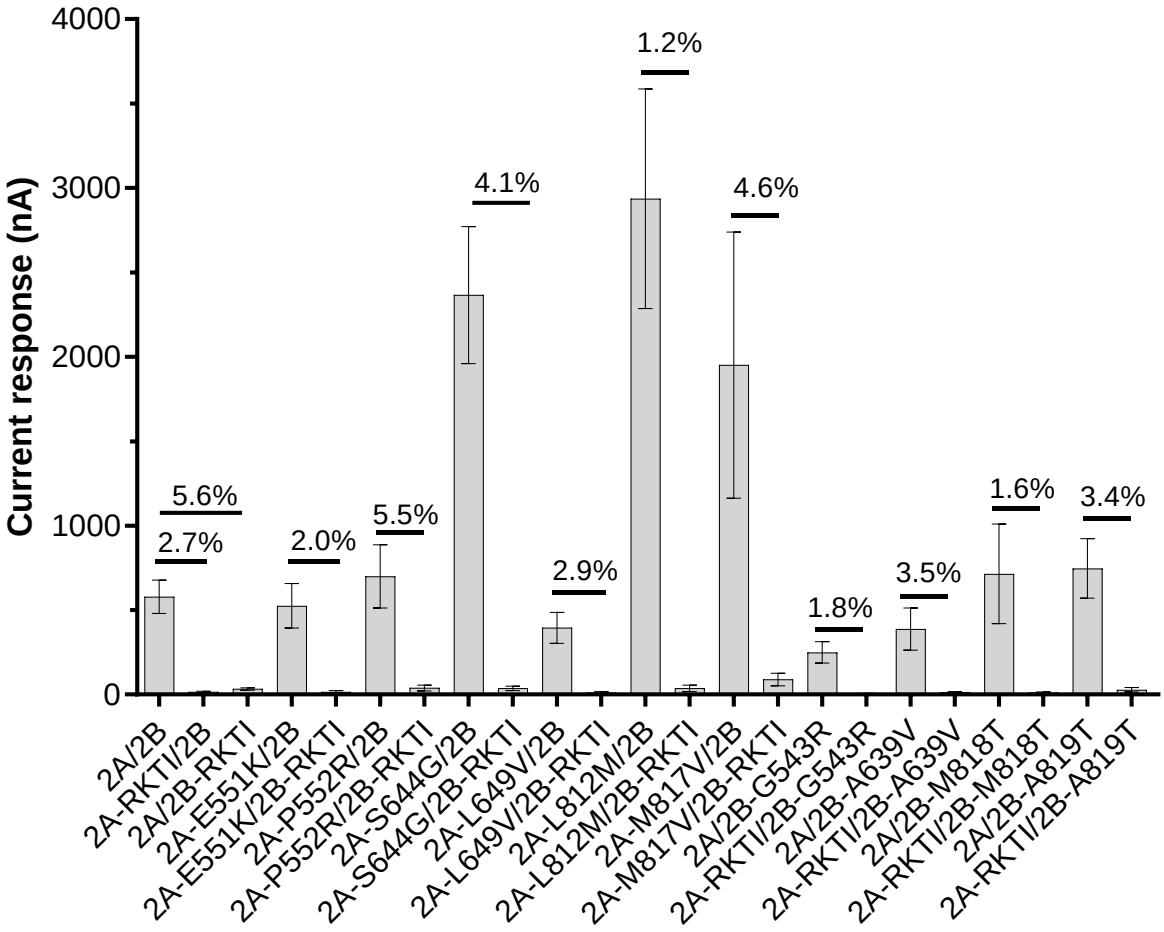

Supplemental Figure S1: The mean raw current ± SEM in nanoamperes (nA) in response to exposure of *Xenopus* oocytes recorded under two electrode voltage clamp to 100 μM glutamate and 100 μM glycine. Values are given for wild type (2A/2B) or variant GluN1/GluN2A$_{C1}$/GluN2B$_{C2}$ triheteromeric NMDARs that have a wild type agonist binding domain or harbor the RKTI mutations in the agonist binding domain that render the GluN2 subunit incapable of binding glutamate (see *Methods*). The current response for RKTI mutations is expressed as a percentage of that observed for NMDARs with functional glutamate binding sites. This percentage is an estimate of the amount of current that could potentially reflect diheteromeric receptors that escape the ER retention strategy we employed and reach the surface with two copies of either the GluN2$_{C1}$ or two copies of GluN2$_{C2}$ subunit (see Hansen et al., 2014).

Supplemental Figure S2

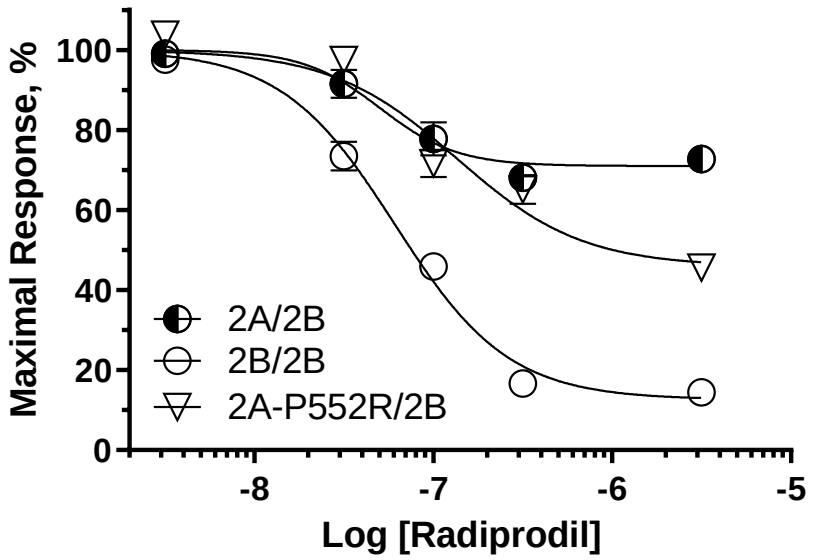

Supplemental Figure S2: Radiprodil inhibition of triheteromeric 2A-P552R/2B NMDA receptors expressed in *Xenopus* oocytes recorded under two electrode voltage clamp to at V_{HOLD} of -40 mV. Radiprodil was applied once, as a single concentration for 3 min to each oocyte, to maximally activated (100 μM glutamate, 100 μM glycine) NMDA receptors. Each data symbol is the mean ± S.E.M of n=10-14 oocytes for 2A-P552R/2B receptors, 10-16 oocytes for 2A/2B receptors, and 9-18 oocytes for 2B/2B receptors. The IC_{50} values for radiprodil inhibition of 2B/2B receptors was 61 nM (87% maximum inhibition), for 2A/2B receptors was 50 nM (29% maximum inhibition), and for 2A-P552R/2B receptors was 135 nM (54% maximum inhibition).